2012

DEPARTAMENTO DE CIÊNCIAS DA VIDA

FACULDADE DE CIÊNCIAS E TECNOLOGIA
UNIVERSIDADE DE COIMBRA

Analysis of the antimicrobial content of amphibian skin secretions and structural and functional characterization of a novel member of the temporin family (temporin-SHe)

Sónia Maria Costa André

2012

Structural and functional characterization of temporin-SHe

Sónia Maria Costa André

DEPARTAMENTO DE CIÊNCIAS DA VIDA

FACULDADE DE CIÊNCIAS E TECNOLOGIA
UNIVERSIDADE DE COIMBRA

Analysis of the antimicrobial content of amphibian skin secretions and structural and functional characterization of a novel member of the temporin family (temporin-SHe)

Dissertação apresentada à Universidade de Coimbra para cumprimento dos requisitos necessários à obtenção do grau de Mestre em Biologia Celular e Molecular, realizada sob a orientação científica do Professor Doutor Ali Ladram (Universidade de Pierre et Marie Curie, France) e do Professor Doutor Paula Veríssimo (Universidade de Coimbra)

Sónia Maria Costa André

2012

AKNOWLEDGMENTS

I owe sincere and earnest thankfulness to Professor Thierry Foulon for warmly welcoming me in his laboratory, as well as all the team for their friendship, support and cheerfulness, providing me an excellent atmosphere for doing research.

I offer my sincerest gratitude to my supervisor, Dr. Ali Ladram, who has supported me, and for his availability, patience, knowledge and care along this internship.

I would like to thanks also my co-supervisor, Dr. Paula Veríssimo, for her confidence in me during this year and for advising and supervising me.

I am also indebted to François Lemoine who took care of "my frogs" *Trachycephalus resinifictrix*, allowing me to study them.

I would like to show my gratitude to the PhD student Zahid Raja, for helping me with his technical advices and for performing leishmanicidal and cytotoxic assays in collaboration with Dr. Bruno Oury and Dr. Denis Sereno.

I would like also to show my gratitude to Amandine Anastasio, Louis Guibout and Christophe Piesse. They cheer me up and stood by me through good and bad times.

Finally, I would like to thank my family, specially my mother for supporting me through the duration of my studies and for her encouragement and endless love.

ABSTRACT

The growing problem of resistance to conventional antibiotics and the need to develop new compounds with original modes of action has stimulated interest in antimicrobial peptides (AMPs) as substitutable pharmaceuticals. AMPs are key components of the innate immune system of several organisms (from microorganisms to vertebrates), acting as the first line of host defense against pathogens. Amphibian skin secretions represent one of the richest natural sources of AMPs. Indeed, 50.6% of antibacterial peptides reported in the Antimicrobial Peptide Database (http://aps.unmc.edu/AP/main.php) come from amphibians. Thus, amphibian skin represents a good model for the identification of novel potent AMPs with therapeutic potential and for studying the mechanism of action of these peptides.

The first aim of my Master 2 internship was to analyze the AMP content of frogs of the subfamily Hylinae which have been very poorly studied, and particularly those of the genus *Trachycephalus* which were not studied. *Trachycephalus resinifictrix* is a South American tree frog (family Hylidae, subfamily Hylinae) also referred to as Amazon Milk Frog because of its milky and poisonous secretions when threatened. Through bioguided fractionation of its skin secretions, antibacterial activity against *Staphylococcus aureus* was detected in HPLC fractions. We attempt to identify the active compounds by tandem mass spectrometry (MS/MS) on a fraction displaying high inhibitory bacterial growth activity. However, no sequence information was obtained due to insufficient material.

The second aim was to characterize the structure and function of temporin-SHe, a small AMP (16 residues) from a North African ranid frog (*Pelophylax saharica*) that was recently identified by the host team by molecular cloning of the precursor. We have produced temporin-SHe by solid phase peptide synthesis and used circular dichroism to investigate its secondary structure. Our results indicated that temporin-SHe can adopt α-helical conformation when bound to negatively charged membranes, while no ordered structure (random coil) is observed for the peptide in solution. In contrast with many members of the Temporin family, temporin-SHe exhibited broad-spectrum antimicrobial activity with high potency against Gram-positive bacteria (including multiresistant *Staphylococcus aureus*) and yeasts (MIC = 1.5-12.5 µM), and to a lesser extent, toward Gram-negative bacteria and *Candida* (MIC = 25-60 µM). Interestingly, temporin-SHe was potent against the promastigote form of the human protozoan parasite *Leishmania* (IC_{50} around 10 µM). A preliminary study using monocytes as mammalian cells revealed that temporin-SHe was more cytotoxic (LC_{50} = 21 µM) than temporin-SHd (LC_{50} = 66 µM). We have shown that bactericidal activity of temporin-SHe was correlated with membrane permeabilization of bacteria. Moreover, a strong disturbance of the membrane bilayer was induced upon interaction of the peptide with negatively charged phospholipid vesicles (differential scanning calorimetry studies).

The short length, high potency, and broad-spectrum activity of temporins-SH, suggest them as good candidates for the development of therapeutic antimicrobial agents with new mode of action, although pharmacomodulation is needed to improve their therapeutic index (LC_{50}/MIC ratio). To date, very few AMPs, including only four temporins (A, B, SHa and SHd), are active against parasites. Our results indicate that temporin-SHe represents a valuable additional tool for understanding the antiparasitic mechanism of action of AMPs, which still remains unknown.

Keywords: *Amphibians, antimicrobial peptides, bioguided fractionation, temporin-SHe, structure/activity/mechanism.*

RESUMO

O problema da resistência aos antibibióticos convencionais e a necessidade de desenvolver novos compostos com diferentes modos de ação, têm estimulado o interesse em péptidos antimicrobianos (PAMs) como possíveis pharmacêuticos de substituição. Os PAMs são componentes-chave do sistema imunitário inato de vários organismos agindo como a primeira linha de defesa contra patogénios. As secreções de pele dos anfíbios representa uma fonte rica em PAMs. De facto, segundo a base de dados *Antimicrobial Peptide Database* (http://aps.unmc.edu/AP/main.php), 50,6% dos péptidos antibacterianos provêm de anfíbios. Assim, a pele de anfíbio representa um ótimo modelo para a identificação de novos PAMs com potencial terapêutico e para estudar o mescanismo de ação destes.

O primeiro objetivo da minha tése de mestrado era analisar o conteúdo em PAMs a partir de *Trachycephalus resinifictrix*, uma rã arborícola da América do Sul (família Hylidae, subfamília Hylinae) pertencente ao género *Trachycephalus*, e que nunca foi estudada. Através do fracionamento bioguiado das suas secreções, uma actividade antibacteriana contra *Staphylococcus aureus* foi detectada em frações de HPLC. Por espectrometria de massa em *tandem* (MS/MS) numa fração de HPLC que mostrava uma potente actividade antibacteriana, tentamos identificar os compostos ativos. No entanto, devido à fraca quantidade de material nenhuma informação de sequência foi obtida.

O segundo objetivo era a caracterização estrutural e funcional da temporin-SHe, um pequeno PAM (16 resíduos) proveniente da rã Norte Africana *Pelophylax saharica* (família Ranidae), identificado recentemente pela equipa por clonagem molecular do precursor. Este péptido foi sintetizado em fase sólida e a técnica de dicroísmo circular foi utilizada para investigar a sua estrutrura secundária. Os nossos resultados indicam que a temporin-SHe adota uma estrutura em hélice-α quando associada a membranas carregadas negativamente, sendo não estrurada em solução. Em contraste com outros membros da família das Temporins, a temporin-SHe exibiu um largo espectro antimicrobiano com uma elevada atividade contra bactérias Gram-positivas (incluindo *Staphylococcus aureus* multiresistentes) e leveduras (CMI = 1,5-12,5 μM), e em menor extensão, contra bactérias Gram-negativas e *Candida* (CMI = 25-60 μM). De maneira interessante, a temporin-SHe mostrou-se também ativa contra a forma promastigote do parasita *Leishmania* (IC_{50} à volta de 10 μM). Um estudo preliminar usando monócitos como células mamíferas revelou que a temporin-SHe era mais citotóxica (LC_{50} = 21 μM) que a temporin-SHd (LC_{50} = 66 μM). Mostramos igualmente que a atividade bactericida da temporin-SHe estava correlacionada com a permeabilização da membrana bacteriana. Adicionalmente, uma forte perturbação da camada lipídica foi induzida após interação do péptido com vesículas phospholipídicas carregadas negativamente.

O pequeno tamanho, a elevada potência, e o largo espectro de atividade das temporins-SH, suggerem-nas como potentes candidatos para o desenvolvimento de agentes terapêuticos com novos modos de ação, embora seja necessário amelhorar o índice terapêutico (razão LC_{50}/CMI). Presentemente, pouco PAMs, incluindo somente 4 temporins (A, B, SHa e SHd) são ativos contra os parasitas. Os nossos resultados indicam que a temporin-SHe representa uma ferramenta adicional valiosa para a compreensão do mecanismo de ação anti-parasitário dos PAMs, que ainda permanece desconhecido.

***Palavras-Chave**: Anfíbios, péptidos antimicrobianos, fracionamento bioguiado, temporin-SHe, estrutura/atividade/mecanismo.*

INDEX

ABBREVIATIONS

ACN: Acetonitrile

AMPs: Antimicrobial peptides

APD: Antimicrobial Peptide Database (http://aps.unmc.edu/AP/main.php)

BHI: Brain heart infusion

CD: Circular dichroism

CFU: Colony-forming unit

CL: Cardiolipin

DEPC: Diethylpyrocarbonate

DMPC: Dimyristoyl phosphatidyl choline

DMPG: Dimyristoyl phosphatidyl glycerol

dNTPs: Deoxynucleotide triphosphates

DPC: Dodecylphophocholine

DRP: Dermaseptin-related peptide

DRS: Dermaseptin

DSC: Differential scanning calorimetry

HIV: Human immunodeficiency virus

IPTG: Isopropyl β-D-1-thiogalactopyranoside

LB: Luria-Bertani

LPS: Lipopolysaccharides

LUVs: Large unilamellar vesicles

MALDI-TOF: Matrix-assisted laser desorption/ionization-time of flight

MH: Mueller-Hinton

MIC: Minimal inhibitory concentration

MLVs: Multilamellar vesicles

MMLV: Moloney-Murine Leukemia Virus

MS/MS: Tandem mass spectrometry

ONP: Ortho-nitrophenol

ONPG: Orthonitrophenyl-β-D-galactopyranoside,

PBS: Phosphate buffered saline

PC: Phosphatidylcholine

PCR: Polymerase chain reaction

PE: Phosphatidylethanolamine

PG: Phosphatidylglycerol

PS: Phosphatidylserine

RP-HPLC: Reversed-phase high performance liquid chromatography

SDS: Sodium dodecyl sulphate

SM: Sphingomyelin

SOC: Super optimal broth (SOB) with catabolite repression (glucose)

ST: Sterols

TFA: Trifluoroacetic acid

TIS: Triisopropylsilane

UTR: Untranslated region

X-Gal: 5-bromo-4-chloro-3-indolyl-β-D-galactopyranoside

YPD: Yeast Peptone Dextrose

INTRODUCTION

Disease-causing microbes that have become resistant to antibiotic drug therapy are an increasing public health problem. Therefore, there is an urgent need to develop new antibiotic lead compounds with original modes of action. Antimicrobial peptides (AMPs) have raised much interest as a promising class of novel therapeutic agents and a possible alternative to conventional antibiotics.

AMPs are innate immune effectors produced by several organisms, including microorganisms, insects, plants and vertebrates. They kill rapidly a broad spectrum of microorganisms (Gram-negative and Gram-positive bacteria, fungi, protozoa, yeasts and enveloped viruses) by acting through a non-receptor-mediated membrane lytic mechanism that limits the induction of microbial resistance [1]. AMPs also operate as immunomodulators through direct interactions with host cells and modulation of the inflammatory/immune processes (cytokine release, angiogenesis, chemotaxis, wound healing, cell proliferation…) [2, 3].

Amphibian skin secretions are one of the richest sources of natural broad-spectrum antimicrobial peptides. Approximately 40% of AMPs reported in The Antimicrobial Peptide Database (APD, http://aps.unmc.edu/AP/main.php) [4] belong to amphibians. Several other pharmacologically active compounds are also present in the amphibian skin such as biogenic amines, bufogenines, steroids, alkaloids, peptides and proteins [5, 6]. Many of the amphibian peptides have their counterparts in tissues with the same embryonic-ectodermal origin, such as mammalian gastrointestinal tract and brain, leading to the concept of the existence of a brain-gut-skin peptide triangle (reviewed in [7]). The basis of this hypothesis is that a peptide found in one of these compartments (amphibian skin, mammalian brain or gut) should also be present in the other two, with a similar or identical structure [8]. This observation has provided further stimulus to the study of frog-skin peptides [7], and particularly AMPs which has prompted an interest over the last few decades.

1. Classification of amphibians

Amphibia is a class of tetrapod vertebrates that contains about 6771 living species already described and distributed among three orders, including Anura (frogs and toads, 5966 species), Caudata (salamanders, 619 species) and Gymnophiona (caecilians, 186 species) [9, 10]. The first one is divided into 49 families, which are themselves divided into subfamilies (figure 1) [9].

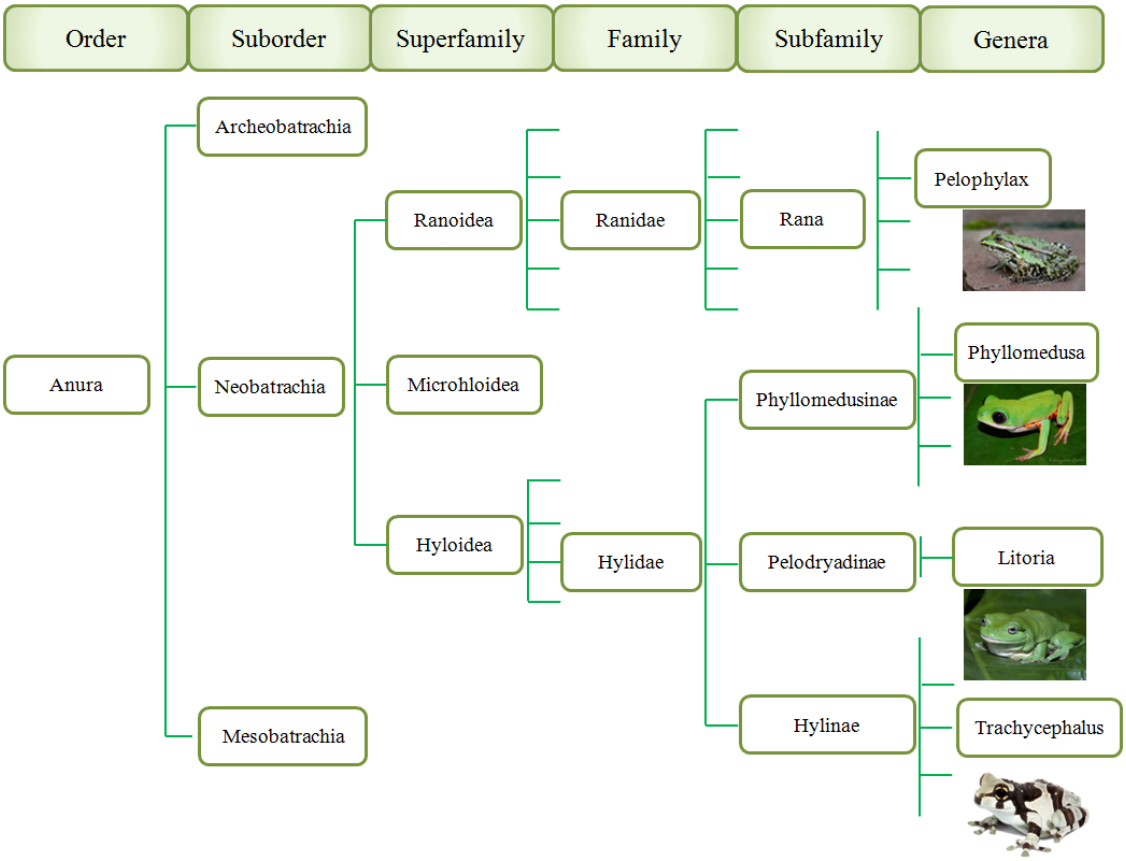

Figure 1: Brief classification of amphibians belonging to the order Anura. Only some subfamilies (Rana, Phyllomedusinae, Pelodryadinae and Hylinae) are represented.

2. Dermal glands of amphibians

Amphibians have established the transition between aquatic and terrestrial environments due to a gradual acquisition of a set of physiological and morphological adaptations, such as the presence of a highly specialized integument – the skin [10].

The anuran skin exhibits morphofunctional diversity adapted to a number of adverse factors present in the species habitat environment [11]. Generally, the frog skin contains three types of cutaneous glands (figure 2), which differ in size, distribution and secretory activity [12, 13]. The lipid glands (figure 2 A) promote the impermeabilization of the skin in order to decrease water loss and are localized mostly in the dorsal and dorsolateral regions [12]. The mucous glands (figure 2 A), which usually are smaller and more numerous, secrete mucins in order to maintain skin lubrification, moisture and thermoregulation and to prevent mechanical damage [5, 13, 14]. For some amphibians, these glands are also involved in reproduction and defense (reviewed in [14]) and are fairly abundant in the ventral surface skin [12]. The third type of glands is the serous or granular glands (also called venom glands) (figure 2 A-C) formed by syncytial cells, with the nuclei located at the periphery of the syncytium [7]. These glands are widely distributed on the dorsal/dorsolateral cutaneous region and are responsible for the synthesis and storage of a wide range of noxious or toxic compounds which provide protection against bacterial and fungal infections, as well as predators [12, 14]. Their cytoplasm is rich of peptide-containing secretory granules, which fill the totality of the gland (figure 2 B). Upon external stimuli, a massive granule discharge is induced by a holocrine-like mechanism involving the contraction of myoepithelial cells surrounding the glands (figure 2 C) [7, 11]. Approximately 15 days are needed to refill the gland with secretory granules.

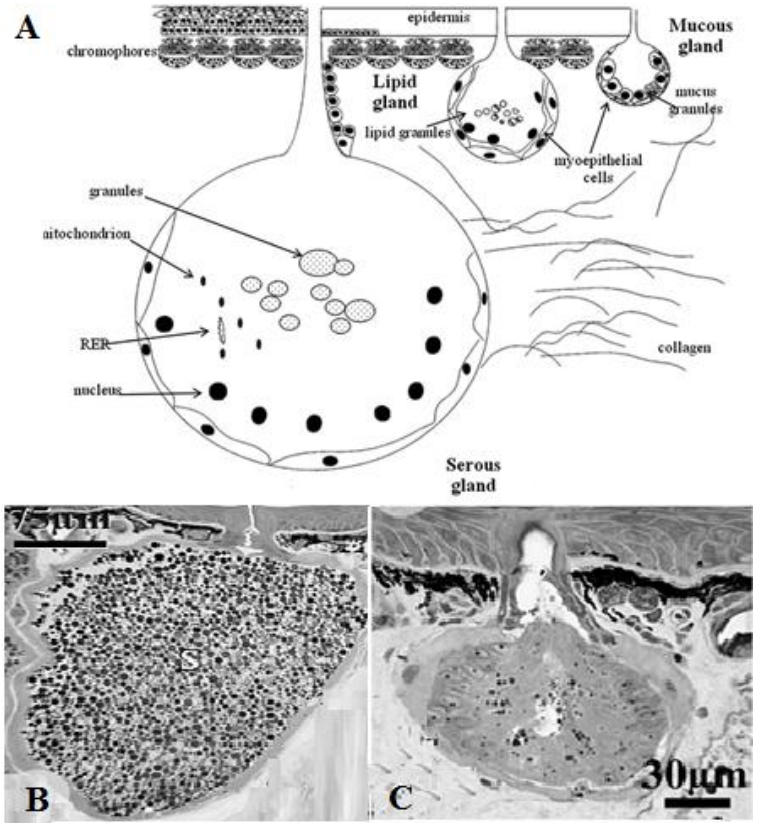

Figure 2: Representation of dermal glands of amphibians. A) Scheme of dermal glands from the skin of *Phyllomedusa bicolor* showing the three types of glands (mucous, lipid and serous) [15]. B-C) Light microscope observations of serous cutaneous gland from *Trachycephalus venulosa*. B) The entire syncytial cytoplasm is filled with dense secretory granules. C) Serous depletion of the secretory granules after external stimuli, indicating a massive granule discharge (adapted from [16]).

3. Antimicrobial peptide biosynthesis in amphibian skin

AMPs are synthesized as prepropeptides (ribosomal pathway) in the multi-nucleated cells of the granular glands of the skin (figure 3) [17]. The canonical precursor architecture comprises a common N-terminal preprosequence that is remarkably well conserved both within and between species and a C-terminal region corresponding to the mature AMP progenitor sequence that varies markedly. The conserved region contains a signal peptide followed by an acidic intervening sequence that ends in a typical prohormone processing signal Lys-Arg (KR) [17, 18]. The signal sequence is necessary to correctly target the precursor to the rough endoplasmic reticulum. After its elimination by a signal peptidase in the endoplasmic reticulum lumen, post-translational modifications (proteolytic processing, C-terminal amidation, amino acid isomerization…) occur in the

trans-Golgi and the secretory granules to release the AMP progenitor sequence from the precursor and to yield the biologically active AMP [18-21].

The pattern of conserved and variable regions in skin antimicrobial peptide precursors is the opposite of that of conventional secreted peptides, suggesting that the conserved preproregion is important for the biology of the expressing cell [22].

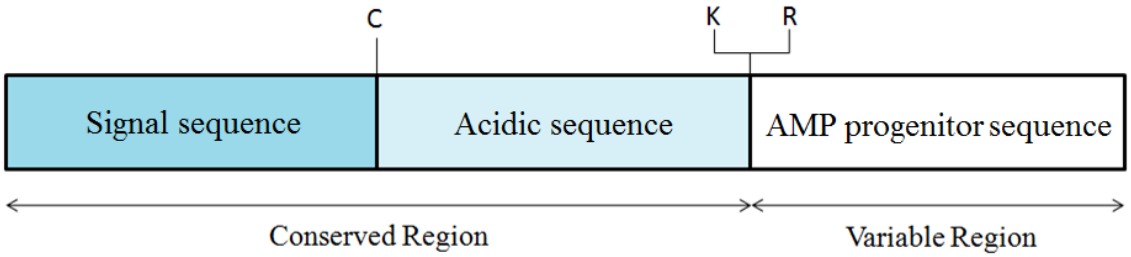

Figure 3: Schematic representation of amphibian AMP precursor. This precursor contains a highly conserved N-terminal region (signal sequence and acidic sequence) and a variable C-terminal region corresponding to the AMP progenitor sequence. The mature AMP is released after proteolytic processing at the dibasic amino acid site (KR) and can undergo post-translational modifications, such as C-terminal amidation for example.

Moreover, this pattern makes the precursors of AMPs belonging to the dermaseptin superfamily one of the most extreme examples observed to date for homologous gene products within a single order of organisms. The conservation is not limited to the coding region of the corresponding mRNAs but also extends into the 5'- and 3'-untranslated regions [23]. This reinforces the existence for theses precursors of a high sequence conservation surrounded by a region of high sequence variability [24].

Most of the AMPs from ranid and hylid frogs are preprodermaseptin-derived products (figure 4), such as for example, the brevinin-1 and -2 families, esculentins-1 and -2, ranatuerins-1 and -2, ranalexins and temporins (frogs of the family Ranidae), and dermaseptins B, dermaseptin-related peptides (DRP), phylloxins, dermatoxins and caerins (frogs of the family Hylidae) (reviewed in [22]). Interestingly, preprodermaseptins from hylid frogs also encode non-antimicrobial peptides, such as dermorphins, deltorphins and dermenkephalins, opioid heptapeptides containing a D-amino acid residue, which are very potent and specific agonists of μ or δ-opioid receptors [25]. The high similarity of preproregions of precursors that result in structurally diverse end-products in distantly related amphibians suggests that the corresponding genes all came from a common ancestor [23].

Targeted hypermutation of the C-terminal antimicrobial-coding region of preprodermaseptin genes might have evolved as a way of increasing genetic diversity and so accelerating the adaptation of frogs to noxious microbial fauna with a maximum protection against a large range of pathogens [17, 24].

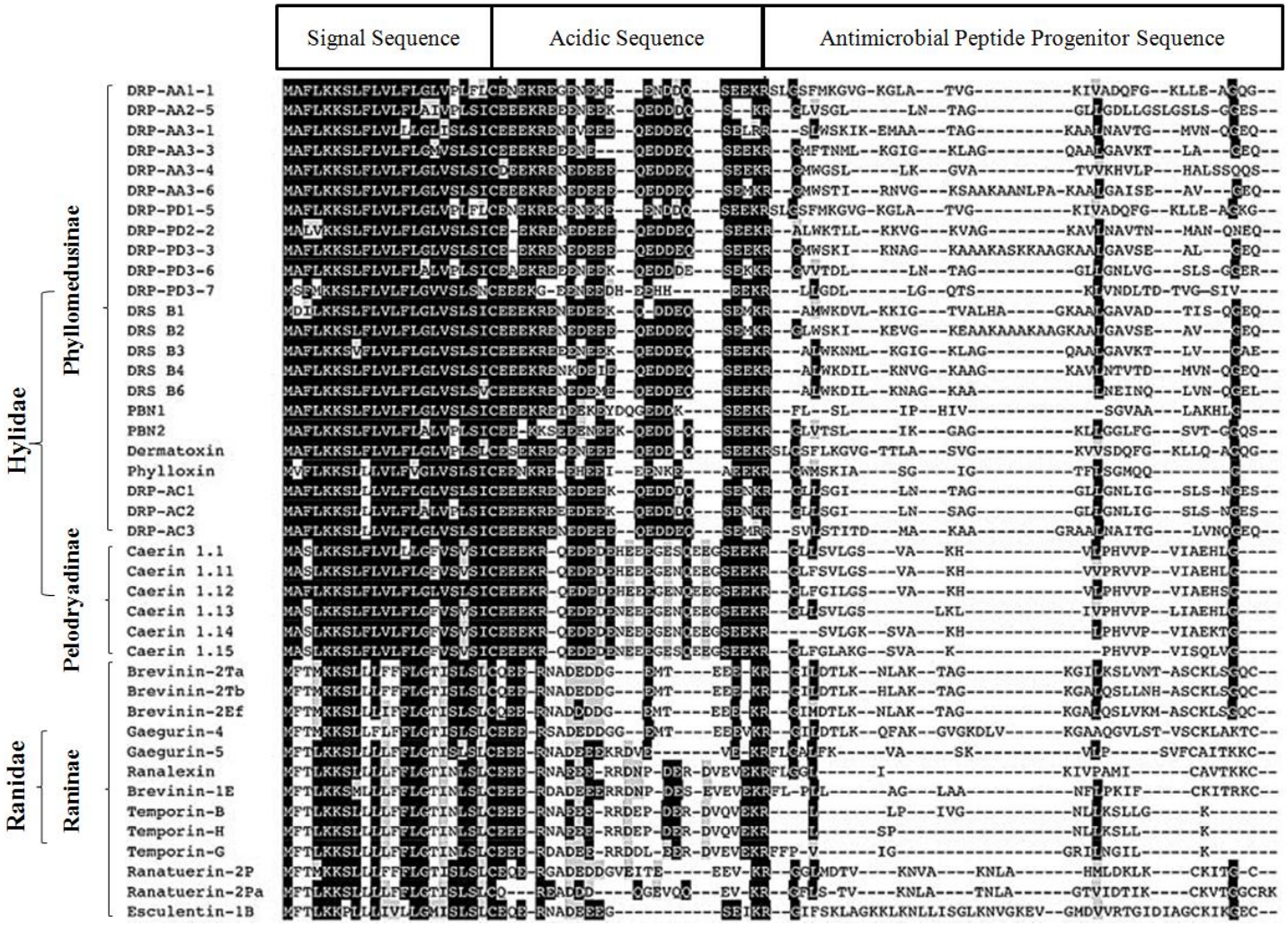

Figure 4: Conserved preproregion and hypervariable antimicrobial domain of preprodermaseptins. Alignment of the predicted amino acid sequences (single-letter code) of preprodermaseptin cDNAs obtained from hylid and ranid frogs, including the signal sequence, the acidic propiece and the antimicrobial peptide progenitor sequence. Gaps (-) have been introduced to maximize sequence similarities. Identical (black background) and similar (shaded background) amino acid residues are highlighted. Among the hylid sequences, DRS, dermaseptin B from *P. bicolor*, DRP, dermaseptin-related peptide (appended with AA, AC or PD to indicate that the sequences were identified from *A. annae*, *A. callidryas* and *P. danicolor*, respectively). Among the ranid sequences, temporins B, H and G and brevinins 2Ta and 2Tb are from *R. temporia*, brevinins 1E and 2Ef and esculentin 1B from *R. esculenta*, ranalexin from *R. catesbeiana*, gaegurins 4 and 5 from *R. rugosa*, and ranatuerin-2P and 2Pa from *R. pipiens*. Raninae, Pelodryadinae and Phyllomedusinae are subfamilies belonging to the family Ranidae (the first one) and the family Hylidae (the other two). (adapted from [24]).

4. Structures of amphibian antimicrobial peptides

Natural amphibian skin antimicrobial peptides comprise between 8 and 100 amino acid residues and usually have a net positive charge at physiological pH (ranging from +1 to +30) due to the presence of multiple lysine and arginine residues [4, 26-28]. These molecules are hydrophobic and usually amphipathic, with a hydrophobic face containing non-polar amino acid side-chains and a hydrophilic face with polar and positively charged residues [27, 28].

Amphibian AMPs belong mainly to these two structure classes:

- Linear α-helical peptides without cysteine residues - These AMPs are unstructured in aqueous solutions whereas they have the propensity to form an amphipatic α-helix in the presence of phospholipid vesicles or in a membrane-mimetic solvent such as sodium dodecyl sulphate (SDS) micelles [29, 30]. For example, magainins (from *Xenopus*), caerins (from *Litoria*) and dermaseptins (from *Phylomedusa*) belong to this structural class (figure 5) [29, 31].

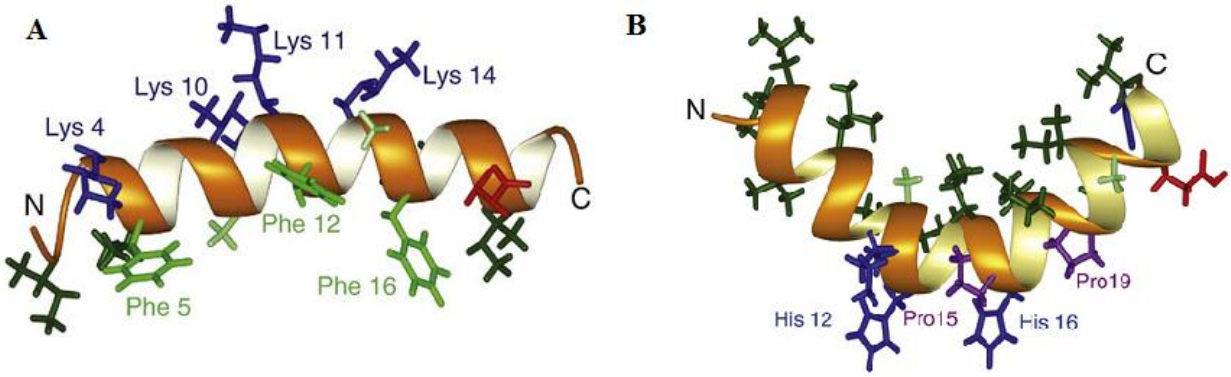

Figure 5: α-helical structure of magainin 2 (A) and caerin 1.1 (B) bound to dodecylphosphocholine (DPC) micelles. Hydrophobic amino acids are colored in shades of green (Phe, Trp in green; Ile, Val, Leu in dark green; Ala in pale green), cationic residues are indicated in blue and anionic residues are shown in red [31].

- Peptides with β-hairpin-like structure and cysteine residues - These AMPs contain a C-terminal loop stabilized by an intramolecular disulfide bond. This region is also called "Rana box" because many such structured AMPs are present in ranid frogs, like esculentins, ranalexins, brevinins and gaegurins, for example (figure 6) [29, 31, 32]. Like α-helical peptides, these AMPs are unfolded in aqueous solutions but the N-terminal can adopt an amphipathic α-helical conformation in hydrophobic environments, depending on the size of this segment and its hydrophobicity [32, 33].

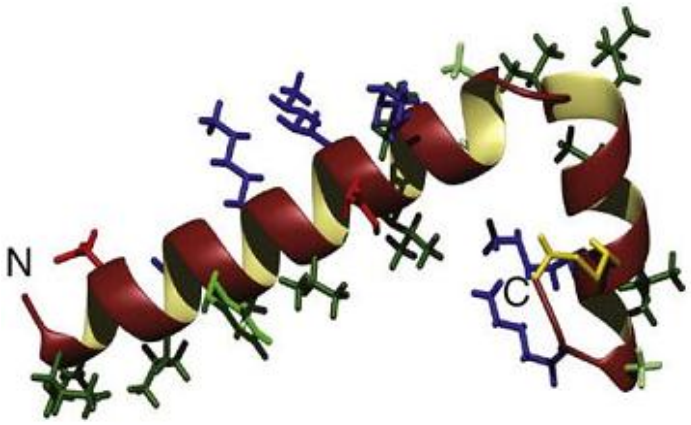

Figure 6: Solution structure of gaegurin-4 in 80 % deuterated methanol. Hydrophobic amino acids are colored in shades of green (Phe, Trp in green; Ile, Val, Leu in dark green; Ala in pale green), cationic residues are indicated in blue and anionic residues are shown in red. The C-terminal disulfide bond is colored in gold. Note that the N-terminal has a α-helical conformation [31].

5. Mechanism of action of antimicrobial peptides

AMPs from amphibians exhibit a broad-spectrum activity and can kill aerobic and anaerobic Gram-positive and Gram-negative bacteria, yeast, filamentous fungi, protozoa, viruses and tumor cells (Table 1). These peptides may have synergistic effects, which increase their effectiveness, and also hemolytic activity [32]. Today, there are 1997 antimicrobial peptides reported in the database APD, of which 1601 are antibacterial (80.17%) (Table 1) with approximately 50% coming from amphibians (figure 7) [4].

Table 1: Biological activities of AMPs. There are 1997 AMPs reported in the Antimicrobial Peptide Database (APD) with 80.17% being antibacterial. Total percentage is above 100% due to the fact that an AMP may have several activities (i.e. antibacterial, antifungal and antiviral for example) [4].

AMPs reported in the Antimicrobial Peptide Database (APD)		
Activity	**Number**	**Percentage**
Antibacterial peptide	1601	80.17%
Antifungal peptide	698	34.95%
Antiviral peptide	122	6.10%
Anticancer peptide	140	7.01%

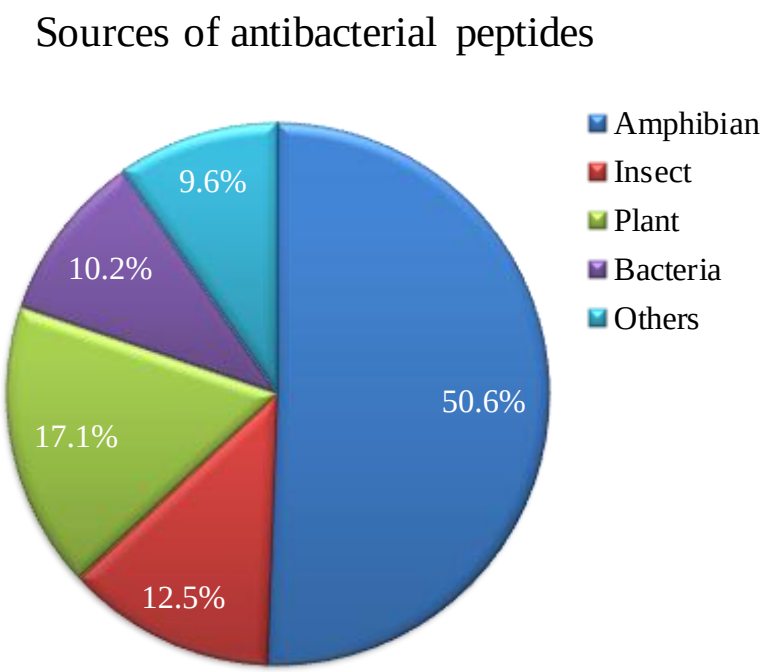

Figure 7: The different sources of antibacterial peptides. A great part (50.6%) comes from amphibians [4].

The exact mechanism by which AMPs exert their killing actions is not completely understood, but a common property is their interaction with the phospholipids of the cytoplasmic membrane, leading to permeabilization and subsequently lysis of the cell [33]. However, how AMPs can selectively distinguish between microbial and host cytoplasmic membranes?

5.1. Membrane composition

The biological membrane is a fluid structure with various proteins embedded in or attached to a bilayer of phospholipids (fluid mosaic model). In some organisms like eukaryotes, sterols and glycerides also contribute to the topology surface and biochemical architecture of biomembranes [26]. Differences between microbial and host membranes exist. In fact, bacterial membranes are predominantly composed of negatively charged phospholipids, such as phosphatidylglycerol (PG), cardiolipin (CL) or phosphatidylserine (PS), which gives to whole membrane an electronegative net charge [26]. In addition, the outer surface of Gram-negative and Gram-positive bacteria contains lipopolysaccharides (LPS) and acidic polysaccharides (teichoic acids), respectively, that enhance the electronegative charge of biomembranes (rewieved in [34]). In contrast, mammalian cytoplasmic membranes have usually a neutral net charge because they are mainly composed of zwitterionic phospholipids, such as phosphatidylethanolamine (PE), phosphatidylcholine (PC) or sphingomyelin (SM), as well as sterols (cholesterol) [26]. In figure 8, we can see that phospholipid composition and asymmetry of the cytoplasmic membrane differ considerably between microorganisms and mammalian cells. Since AMPs are mostly cationic and bind preferentially to anionic lipids, these differences are believed to account for the molecular basis of the affinity/selectivity (microorganism versus host cells) of AMPs [26, 35].

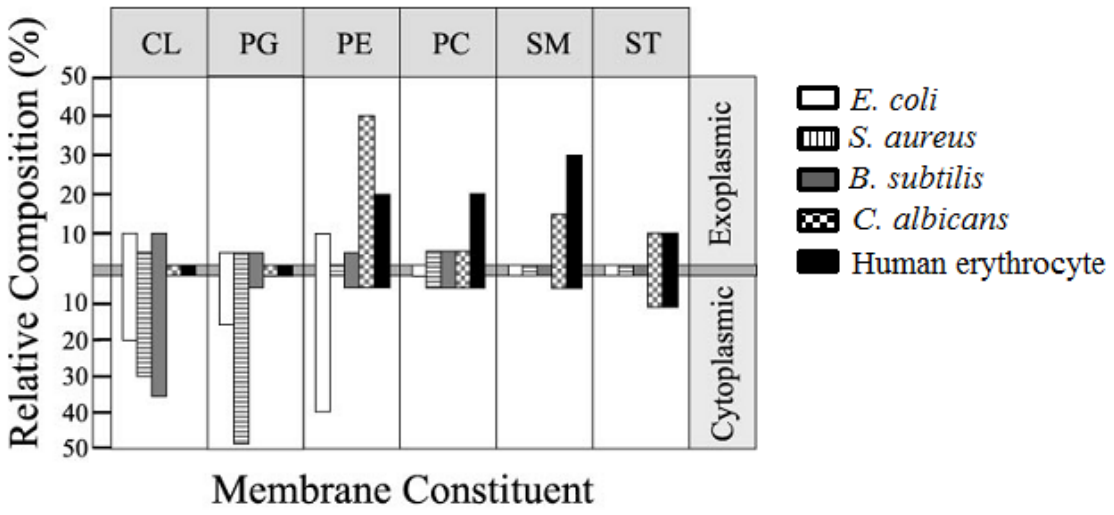

Figure 8: Comparative architecture of microbial and mammalian cytoplasmic membranes. The relative composition and distribution between inner and outer membrane leaflets are indicated for cytoplasmic microbial (*E. coli*, *S. aureus*, *B. subtilis*, *C. albicans*) and mammalian (human erythrocyte) membranes. CL: cardiolipin; PG: phosphatidylglycerol; PE: phosphatidylethanolamine; PC: phosphatidylcholine; SM: sphingomyelin and ST: sterols (cholesterol or ergosterol). (adapted from [26]).

Another important factor for the selectivity of AMPs toward microbial cells is the transmembrane potential ($\Delta\psi$), an electrochemical gradient determined by extents and rates of proton flux across the membrane [26]. Normal mammalian cells exhibit a $\Delta\psi$ ranging from -90 to -110 mV, whereas a $\Delta\psi$ of -130 mV to -150 mV is observed for bacteria in logarithmic phase growth [26].

As a result, antimicrobial activity and selective toxicity of a peptide against pathogens is determined by a complex interaction between parameters such as conformation, charge, hydrophobicity and amphipathicity [26].

Several studies on both live organisms and model membranes have indicated that most AMPs induce plasma membrane permeabilization by mechanisms involving the formation of transmembrane pores (barrel-stave and wormhole models) or micellization of the cytoplasmic membrane by a detergent-like action (carpet model).

5.2. Barrel-stave model

The barrel-stave mechanism describes the formation of transmembrane channels/pores by bundles of amphipathic α-helices peptides, where their hydrophobic surfaces interact with the lipid core of the membrane and their hydrophilic surfaces point inward, producing an aqueous pore (figure 9) [36]. Initially, AMP binds to the membrane surface, promoting the transition of the peptide from the random coil to the α-helical conformation (figure 9 A). When bound peptide achieves a threshold concentration, peptides monomers insert into the hydrophobic core of the membrane bilayer, occurring a progressive recruitment of additional monomers to increase the pore size (figure 9 B) [26].

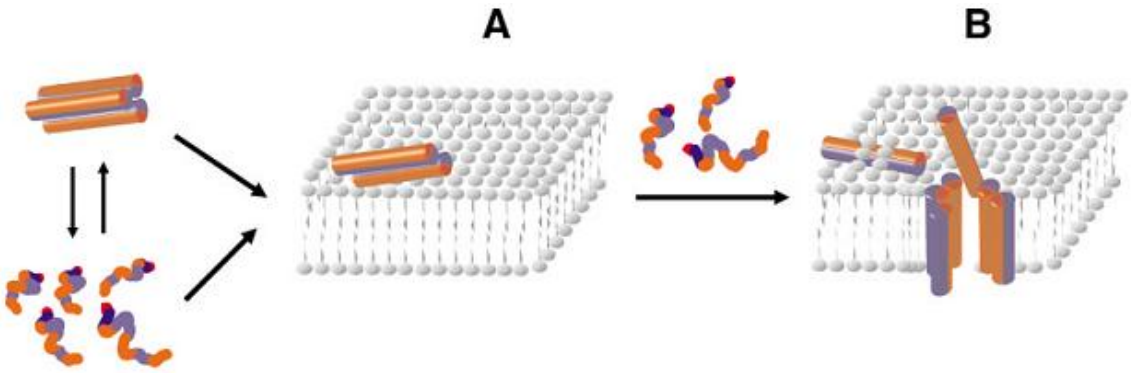

Figure 9: The barrel-stave model. AMPs (either as monomers or oligomers) interact with the membrane and assemble on the surface (A), then insert into the lipid bilayer to form transmembrane pores following recruitment of additional AMP molecules (B). The hydrophobic peptide faces align with the lipid core region and the hydrophilic peptide faces form the interior region of the pore. Hydrophilic and hydrophobic faces of the peptide are shown colored red and blue, respectively [34].

Since these peptides can insert into the hydrophobic core of the membrane, it is logical to presume that such interaction is determined predominantly by hydrophobic interactions [36].

5.3. Carpet model

Carpet mechanism or detergent-like mechanism, as the name suggests, is a mechanism by which cytoplasmic membrane micellization occurs after action of AMPs (figure 10). Initially, the cationic AMP targets the membrane via electrostatic interactions with the anionic phospholipid headgroups, covering the surface in a carpet-like manner (figure 10 A) [29]. When a threshold concentration of peptide is reached, changes in membrane fluidity and/or reductions in membrane barrier properties are observed, leading to the loss of membrane integrity (figure 10 B), and consequently the formation of micelles (figure 10 C) [26]. In contrast to the barrel-stave model, this mechanism does not require a specific peptide structure [37]. Therefore, membrane lysis takes place in a dispersion-like manner that does not engage insertion of peptides into the hydrophobic core of the membrane, and consequently pore formation [26, 36].

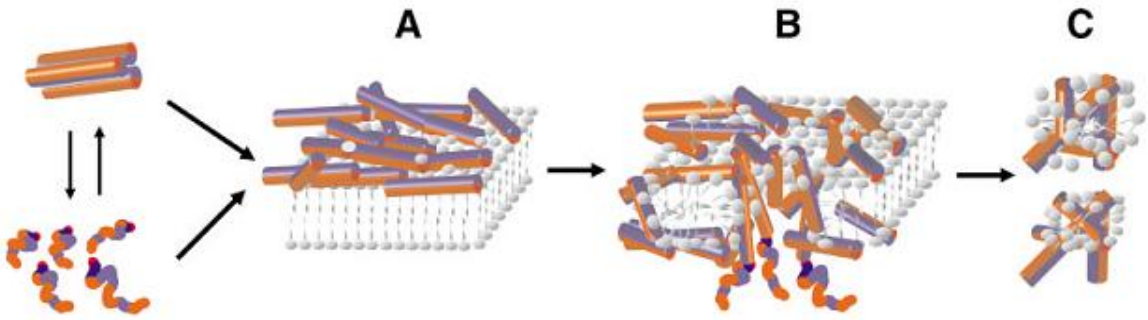

Figure 10: The carpet model. AMPs reach the membrane either as monomers or oligomers, and then bind to the surface of the membrane with their hydrophobic regions facing the membrane and their hydrophilic regions facing the solvent (A). When a threshold concentration is reached, the membrane is permeabilized (B) and membrane lysis occurs with formation of micelles (C). Hydrophilic and hydrophobic faces of the peptide are shown colored red and blue, respectively [34].

5.4. Toroidal model or wormhole mechanism

This model involves both carpeting and pore formation [3], the main difference being the intercalation between lipids and peptides in the transmembrane channel (figure 11) [26]. The α-helical AMP adheres to the outer leaflet membrane, being firstly, oriented parallel to the membrane surface [26]. Once a threshold concentration is reached, peptides begin to self-associate and orient perpendicular to the membrane surface, inducing a positive curvature of the membrane and the formation of a mixed phospholipid-peptide toroidal pore where the hydrophilic face of the peptide remains associated with the polar headsgroups of the phospholipids [38]. Upon dissolution of the pore, in certain cases, peptides can be translocated into the cytoplasm of the target cell where they can interact with potential intracellular targets [3, 26]. This model differs from the barrel-stave model as the peptides are always associated with the lipid head groups even when they are perpendicularly inserted in the lipid bilayer [39].

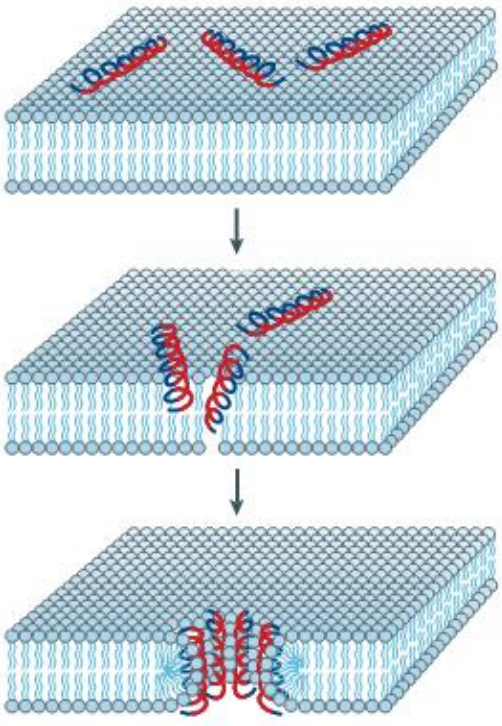

Figure 11: The toroidal or wormhole model. The attached peptides aggregate and induce the lipid monolayers to bend continuously through the pore so that the water core is lined by both the inserted peptides and the lipid head groups. Hydrophilic and hydrophobic regions of the peptide are shown colored red and blue, respectively [29].

In any case, the final result is the permeabilization of the cytoplasmic membrane, and several events can happen like membrane depolarization, outflow of essential metabolites, loss of compositional specificity, exchange with the inner leaflet of the outer membrane, translocation of the peptides to the cytoplasmic side of the membrane where they can interfere with cellular mechanisms, as well as components (reviewed in [40]). All this processes lead to lysis of pathogens [20].

Thus, since AMPs are cidal by targeting the membrane of microorganisms and inducing permeabilization/disruption, it is very difficult for pathogens to develop resistance toward these molecules. This would require a change of the composition and/or organization of the lipid membrane, a probably too expensive solution for the majority of microorganisms [3]. In relation to conventional antibiotics, pathogens become resistant because these drugs act on specific intracellular targets without altering deeply their morphology [26].

6. Antimicrobial peptides from hylid and ranid frogs

6.1. AMPs from frogs belonging to the family Hylidae

Numerous AMPs were identified from different amphibian families. In the present work, we will focus on frogs of the family Hylidae (subfamily Hylinae) and also Ranidae.

The family Hylidae is composed of three subfamilies (Table 2 and 3) [9]:

- Phyllomedusinae, containing 58 species identified today that are divided into 5 genera: *Agalychnis*, *Cruziohyla*, *Phasmahyla*, *Phrynomedusa* and *Phyllomedusa* (Table 2) [9]*;*
- Pelodryadinae, comprising 197 species and only one genus: *Litoria* (Table 2) [9]*;*
- Hylinae, containing 646 species and divided into 40 genera. We will pay more attention to the following genera: *Hyla*, *Pseudis*, *Hypsiboas* and *Trachycephalus* (Table 3) [9].

Phyllomedusinae and Pelodryadinae are the most well-studied hylid subfamilies with more than 80 and 50 AMPs, respectively, identified and characterized (Table 2) [4]. Conversely, very few AMPs were isolated from Hylinae frogs. Indeed, only 8 AMPs were identified from the genera *Pseudis*, *Hyla* and *Hypsiboas* (Table 3) and no information on the precursor sequences is available. This is very surprising considering the large number of species in this subfamily.

Table 2: Phyllomedusinae and Pelodryadinae subfamilies (Hylidae family). The different genera and the different AMPs families are given. An example of a representative member of each AMP family is indicated with its amino acid sequence. As an example, the sequence of the dermaseptin B2 is represented for the Dermaseptin family. For the genus *Litoria*, a non-exhaustive list of AMP families was provided. Amide: C-terminal amidation.

Subfamily	*Genus*	*AMP family*	*Example*	*Sequence*	*Ref.*
Phyllomedusinae	*Agalychnis* *Cruziohyla* *Phasmahyla* *Phrynomedusa* *Phyllomedusa*	Dermaseptins	B2	GLWSKIKEVGKEAAKAAAKAAGKAALGAVSEAV	[41]
		Phylloseptins	L1	LLGMIPLAISAISALSKL$_{amide}$	[42]
		Plasticins	B1a	GLVTSLIKGAGKLLGGLFGSVTG$_{amide}$	[43]
		Dermatoxins	B1	SLGSFLKGVGTTLASVGKVVSDQFGKLLQAGQ	[44]
		Phylloxins	B1	GWMSKIASGIGTFLSGMQQ$_{amide}$	[45]
		Hyposins	H1	LRPAVIRPKGK$_{amide}$	[46]
		Orphan peptides	Dermaseptin S9	GLRSKIWLWVLLMIWQESNKFKKM	[47]
Pelodryadinae	*Litoria*	Aureins	1.2	GLFDIIKKIAESF$_{amide}$	[48]
		Caerins	1.1	GLLSVLGSVAKHVLPHVVPVIAEHL$_{amide}$	[49]
		Citropins	1.1	GLFDVIKKVASVIGGL$_{amide}$	[50]
		Dahleins	1.1	GLFDIIKNIVSTL$_{amide}$	[51]
		Maculatins	1.1	GLFGVLAKVAAHVVPAIAEHF$_{amide}$	[52]
		(…)			

Seven AMP families that are structurally and functionally distinct were characterized from hylid frogs belonging to the subfamily Phyllomedusinae. For example, AMPs from dermaseptin family share a conserved tryptophan (W) residue at position 3 and an AA(A/G)KAAL(G/N)A consensus motif in the midregion.

Conversely, orphan peptides family does not resemble any members of the other peptides families [53].

Table 3: Hylinae subfamily (Hylidae family). Only 4 of the 40 genera are referenced in the present table with all the AMP families identified until today. Amide: C-terminal amidation.

Subfamily	*Genus*	*AMP family*	*Example*	*Sequence*	*Ref.*
Hylinae (646 sp.)	*Pseudis* (9 sp.)	Pseudins	1	GLNTLKKVFQGLHEAIKLINNHVQ	[54]
			2	GLNALKKVFQGIHEAIKLINNHVQ	
			3	GINTLKKVIQGLHEVIKLVSNHE	
			4	GINTLKKVIQGLHEVIKLVSNHA	
	Hyla (35 sp.)	Hylaseptins	P1	GILDAIKAIAKAAG$_{amide}$	[55]
		Hylains	1	GILDAIKAFANALG$_{amide}$	[56]
			2	GILDPIKAFAKAAG$_{amide}$	
	Hypsiboas (84 sp.)	Hylins	a1	IFGAILPLALGALKNLIK$_{amide}$	[57]
	Trachycephalus (12 sp.)			**?**	

As stated earlier, AMPs have a broad-spectrum activity, which can be interesting for therapeutic use. In fact, besides having bactericidal, as well as fungicidal activities, many AMPs have antitumor activity against the major human cancer cell lines and also antidiabetic and antiviral properties [30, 58, 59]. For example, among AMPs listed in Table 2, dermaseptin B2 [58], phylloseptin L1 [42], aurein 1.2 [48], caerin 1.1, citropin 1.1 and maculatin 1.1 [60] are potent antineoplasic peptides. The recognition of cancerous cells from healthy cells is not fully understood. However, many processes have been proposed, such as changes in membrane potential due to higher metabolism, higher exposure of acidic phospholipids in the outer leaflet of membrane, cytoskeleton alterations and possible changes in the extracellular matrix (reviewed in [20]). Furthermore, caerin 1.1, as an example, also has antiviral activity and can inhibits human immunodeficiency virus (HIV) infection of T cells [61]. Ultimately, some

studies realized in rat clonal BRIN-BD11 β-cells demonstrated that pseudin-2 (Table 3) [62], as well as phylloseptin-L2 [59], are able to induce insulin release at concentrations that are not toxic to the cells. Consequently, these peptides could be interesting for treatment of type 2 diabetes [59].

In order to develop new peptide antibiotics with improved therapeutic potential, design strategies and structure-activity relationship studies were used to improve potency and selectivity of AMPs (reviewed in [13]). These modifications might offer significant advantages over natural AMPs as therapeutic agents [63].

Additionally, nanoscale biofunctionalization of biomolecules (i.e. nanobiotechnology) like AMPs is a very promising strategy for applications in the pharmaceutical industry and diagnosis. The interest in AMPs as active materials in bionanostructures is due to their properties, such as the presence of an α-helix structure and positive charges [64]. These structures consist of cationic nanoparticles formed by the conjugation of cholesterol and AMPs that are able to cross blood-brain barrier for treatment of infections, such as fatal *Cryptococcal* meningitis in patients with late-stage HIV infection [65]. These nanoparticules may also be used as sensor elements for detection of *Leishmania* cells [64].

Thus, AMPs appears to be promising candidates as therapeutic agents for the treatment of several diseases.

6.2. AMPs from frogs belonging to the family Ranidae

The family Ranidae is composed of 347 species organized into 16 genera. The genus *Rana* constituted of 48 species of Eurasian and North American frogs [9] was particularly studied. As shown in Table 4, 12 peptide families have been identified from several ranid frog species. Except temporins, all these families contain a C-terminal domain with an intramolecular disulfide bridge called the “Rana box” (figure 6) [1, 66].

In this study, we focus on temporin family, in fact, despite that the others have a broad-spectrum activity against numerous pathogens, as well as insulinotropic properties [67], temporins have characteristics that make them interesting for in-depth investigation of their biological function and mechanism of action.

Table 4: AMP families of ranid frogs. A representative member of each AMP family is indicated with its amino acid sequence [4]. As an example, the sequence of brevinin-1 is given for the Brevinin-1 family. The C-terminal Rana box containing a disulfide bridge is represented in green color. Amide: C-terminal amidation.

Family	*AMP family*	*Example*	*Sequence*
Ranidae	Brevinin-1	1	FLPVLAGIAAKVVPALF**C**KITKK**C**
	Brevinin-2	2	GLLDSLKGFAATAGKGVLQSLLSTAS**C**KLAKT**C**
	Esculentin-1	1	GIFSKLGRKKIKNLLISGLKNVGKEVGMDVVRTGIDIAG **C**KIKGE**C**
	Esculentin-2	2a	GILSLVKGVAKLAGKGLAKEGGKFGLELIA**C**KIAKQ**C**
	Ranatuerin-1	1	SMLSVLKNLGKVGLGFVA**C**KINKQ**C**
	Ranatuerin-2	PLa	GIMDTVKNVAKNLAGQLLDKLK**C**KITA**C**
	Palustrin-2	2a	GFLSTVKNLATNVAGTVLDTIR**C**KVTGG**C**RP
	Japonicin-1	1	FFPIGVF**C**KIFKT**C**
	Japonicin-2	2	FGLPMLSILPKAL**C**ILLKRK**C**
	Nigrocin-2	2	GLLSKVLGVGKKVL**C**GVSGL**C**
	Ranacyclin	T	GALRG**C**WTKSYPPKP**C**K$_{amide}$
	Temporin	A	FLPLIGRVLSGIL$_{amide}$

Initially identified in 1996 in the skin secretion of the frog *Rana temporaria* [66], temporins are among the shortest amphipatic α-helical AMPs found to date, with a single 8-21 amino acid chain. They have a low net positive charge at neutral pH ranging from 0 to +3 and are amidated at their carboxyl end [1]. Temporins are predominantly active toward Gram-positive bacteria, including methicillin- and vancomycin-resistant staphylococci and enterococci, as well as yeasts [66, 68, 69]. They are inactive or weakly active toward Gram-negative bacteria and are generally not toxic to human blood cells at their antimicrobial concentration [66], except for temporin L which has a broad spectrum of activity (Gram-positive and Gram-negative bacteria, yeasts, cancer cells and human erythrocytes) [70]. Furthermore, it has also been demonstrated that some members of the temporin family could have antiparasitic activity. This is the case for temporins A and B, isolated from *Rana temporaria*, and also temporin-SHa (*Pelophylax saharica*) that are active against both the insect (promastigote) and mammalian intracellular stage (amastigote) of the human protozoan parasite *Leishmania*

[71, 72]. Besides their antimicrobial effects, temporins possess additional biological activities. For example, temporin A has chemotactic effects on human phagocytes [73]. Temporins B and L modulate the hydrolytic activity of secretory phospholipase A_2 in human lacrymal fluid, thus improving the efficiency of the immune response to infections [74]. In contrast to many natural AMPs, it was demonstrated that temporins A and B maintain activity in physiological salt concentration, as well as in serum, making them attractive lead compounds for the development of anti-infective drugs [71].

The laboratory has identified several novel members of the temporin family (Table 5) from the North African ranid frog *Pelophylax saharica* (figure 12) using bioguided fractionation of a skin extract combined to mass spectrometry and molecular cloning of the cDNA AMP precursors. These temporins were named temporin-SH (SH for *saharica*) according to the nomenclature proposed for AMPs from the frogs of the family Ranidae [75]. Temporin-SHc (Table 5) is a classical member of the Temporin family with activity against Gram-positive bacteria and yeasts, whereas temporin-SHb is virtually inactive [72]. Interestingly, temporin-SHa (Table 5) displays a potent and broad-spectrum antimicrobial activity, including also Gram-negative bacteria and the parasite of the genus *Leishmania* [72]. Temporin-SHd, -SHe and -SHf were recently identified (Table 5) [76]. The 17-residue long peptide temporin-SHd is also active against *Leishmania* [77] and temporin-SHf, a Phe-rich peptide containing 8 residues, represents the smallest natural AMP characterized today [76].

The structure, activity, and mechanism of action of temporins-SH were well studied [72, 76-78], except for temporin-SHe that was just identified by molecular cloning of the cDNA precursor and remains to be characterized.

Table 5: Sequence and net charge of temporins-SH. Basic residues are indicated (bold, red).

Temporin	Sequence	Number of residue	Net charge (pH 7.4)
SHa	FLSGIVGMLG**K**LF$_{amide}$	13	+2
SHb	FLPIVTNLLSGLL$_{amide}$	13	+1
SHc	FLS**H**IAGFLSNLF$_{amide}$	13	+1
SHd	FLPAALAGIGGILG**K**LF$_{amide}$	17	+2
SHe	FLPALAGIAGLLG**K**IF$_{amide}$	16	+2
SHf	FFFLS**R**IF$_{amide}$	8	+2

7. Purpose of the study

Amphibian skin represents a good model for the identification of novel AMPs with potent activity and therapeutic potential, and for studying the mechanism of action of these peptides.

A first part of my research project was to investigate the AMP content of frogs of the subfamily Hylinae, which have been very poorly studied, and particularly those of the genus *Trachycephalus*. Therefore, we have analyze for the first time by bioguided fractionation the skin secretions of *Trachycephalus resinifictrix*, a South American tree frog also referred to as Amazon Milk Frog because of its milky and poisonous secretions when threatened (figure 12) [79]. Fractionation was performed by semi-preparative and analytical HPLC, and antibacterial activity against *Staphylococcus aureus* was monitored by a liquid growth inhibition assay. We also attempted to characterize the AMP precursors by performing mRNA extraction, RT-PCR and molecular cloning of the cDNAs.

The second part of my Master 2 research project was to perform the structural and functional characterization of temporin-SHe that was previously identified by the host team from the ranid frog *Pelophylax saharica* [76]. We have produced this peptide by solid phase peptide synthesis and determined its structure, antimicrobial activity, and mechanism of action using biochemical and biophysical techniques. Moreover, temporin-SHe was compared to its paralog, temporin-SHd.

Figure 12: *Trachycephalus resinifictrix* (left) and *Pelophylax saharica* (right).

MATERIALS AND METHODS

8. Analysis of antimicrobial peptides from skin secretions of *T. resinifictrix* and molecular cloning of AMP cDNA precursors.

Collection of skin secretions and pre-purification of peptides

Specimens of *Trachycephalus resinifictrix* (2 males and 2 females) were bred and fed crickets by François Lemoine (National Museum of Natural History, MNHN, Paris, France). The temperature was maintained at approximately 25°C and water bowls were provided for bath. Frogs were mildly stressed by electrical stimulation (9 V) and skin secretion was collected, diluted in Milli-Q H_2O and lyophilized.

Lyophilized secretions were dissolved in H_2O containing 0.1% trifluoroacetic acid (TFA), then sonicated for 10 min at 25°C (Ultrasonic cleaner, VWR) and centrifuged (4500 rpm, 20 min, 4°C). The supernatant was lyophilized and dissolved in 0.1% TFA/H_2O in order to obtain a concentration of 1 mg/ml. After sonication for 5 min and centrifugation (16000 x g, 15 min, 4°C), the solution was filtered (0.20 µm) and then loaded onto Sep-Pak C-18 cartridges. After a washing step (0.1% TFA/H_2O), the material was eluted with 60% acetonitrile (ACN) and lyophilized. All these steps were intended to prevent clogging of the HPLC column because of the high viscosity of the sample.

Reversed-phase HPLC (RP-HPLC) fractionation of skin secretions

The lyophilized pre-purified extract (14.5 mg) was reconstituted in 0.1% TFA/H_2O to obtain a concentration of 1 mg/ml, sonicated for 10 min and centrifuged (16000 x g, 10 min, 4°C). Subsequently, the supernatant was lyophilized and dissolved into 6 ml of 20% ACN, followed by sonication for 10 min and centrifugation (13000 x g, 10 min, 4°C). The final supernatant was fractionated by RP-HPLC on a semi-preparative Nucleosil C18 column (5 µm, 250 x 10 mm, Interchim) using a two solvent system: (A) 0.1% TFA/H_2O and (B) 0.07% TFA/ACN.

Elution was performed with a 20-60% linear gradient of solvent B (1%/min) at a flow rate of 4 ml/min. Collected fractions (4 ml) were lyophilized, reconstituted in 500 µl of sterile Milli-Q H_2O and tested for antibacterial activity against the reference strain *Staphylococcus aureus* (see below). In order to improve peaks separation, the active fractions (25, 29 and 37) were rechromatographed on an Uptisphere C18 analytic column (modulo-cart QS, 5 µm, ODS2, 250 x 4.6 mm, Interchim) using a 20-60% linear gradient of solvent B (0.5%/min) at a flow rate of 0.75 ml/min. Major peaks were harvested manually, lyophilized, dissolved into 120 µL of sterile Milli-Q H_2O and tested again against the bacterial strain *Staphylococcus aureus*. Absorbance was monitored at 220 and 280 nm.

Antimicrobial assays

Antibacterial activity of the lyophilized fractions was monitored by a liquid growth inhibition assay against the Gram-positive reference strain *Staphylococcus aureus*. Bacteria were cultured in LB medium for 2-3 h at 37°C with vigorous shaking (250 rpm). After determination of the absorbance at 600 nm (A_{600}), the bacterial culture was centrifuged (1000 x g, 10 min, 4°C), resuspended in MH broth to A_{600} = 0.01 (10^6 cfu/ml) and diluted 80 fold in MH broth (1.25 x 10^4 cfu/ml). Diluted bacteria (50 µl) were mixed with 50 µl of either RP-HPLC fractions or sterile Milli-Q H_2O (negative growth inhibition control) in 96-well microtitration plates. 0.7% formaldehyde was used as positive control. After 18 h of incubation at 37°C with shaking (150 rpm), the bacterial growth was monitored by measuring the change in A_{600} value using a microplate spectrophotometer (Asys Hitech UVM 340). Each assay was performed in duplicate to minimize fraction consume.

The minimal inhibitory concentration (MIC) of synthetic temporin-SHe was determined against Gram-positive bacteria (*Staphylococcus aureus* ATCC 25923, *S. aureus* ST1065, *Enterococcus faecalis* ATCC 29212, *Bacillus megaterium*, *Listeria ivanovii*), Gram-negative bacteria (*Escherichia coli* ATCC 25922, *E. coli* ATCC 35218, *E. coli* ML-35p, *Pseudomonas aeruginosa* ATCC 27853) and yeasts (*Saccharomyces cerevisiae, Candida albicans* ATCC 90028, *C. parapsilosis* ATCC 22019). Bacteria were cultured at 37°C in LB medium and then diluted in MH broth to A_{600} = 0.01 (10^6 cfu/ml), except for *E. faecalis* and *L. ivanovii* which were diluted in LB medium and

BHI, respectively. Yeasts were cultured in YPD medium at 30ºC and diluted in the same medium to A_{600} = 0.01 (10^6 cfu/ml). The MIC was determined by measuring the absorbance at 600 nm in 96-well microtitration plates by growing 50 µl of the microorganism suspension (10^6 cfu/ml) with 50 µl of 2-fold serial dilutions of synthetic temporin-SHe (200-1 µM) 18 h at 37ºC (30ºC for yeasts). MIC was expressed as the lowest concentration of peptide that inhibited bacterial growth completely and as the average value from three independent experiments, each performed in triplicate with positive (0.7% formaldehyde) and negative (without peptide) inhibition control, and sterility control (H_2O).

Mass spectrometry analysis of antibacterial HPLC fractions

HPLC fractions with antibacterial activity were subjected to MALDI-TOF-MS (Voyager DE-Pro, Applied Biosystems – Proteomics and Mass Spectrometry Platform of IFR83, UPMC) in order to determine the mass of the material present in these fractions. Briefly, 1 µl of HPLC fractions were mixed with 1 µl of saturated matrix solution (α-cyano-4-hydroxycinnamic acid) and spotted on a sample plate. The MS positive ion spectra were carried out in the reflector mode with external calibration, using the 4700 Standard Kit (Applied Biosystems).

Isolation of mRNA and reverse transcription

Four adult specimens of *T. resinifictrix* were mildly stressed by electrical stimulation (9 V) and skin secretions were collected with a sterile spatula, diluted in DEPC-treated H_2O and lyophilized. Poly(A)$^+$ RNA was isolated from the lyophilized powder (16.7 mg) using the Micro-FastTrack^{TM} 2.0 mRNA Isolation kit (Invitrogen) according to the manufacturer's protocol. Briefly, 1 ml of lysis buffer[a] supplemented with proteinase K (20 mg/ml) was added to the powder and the solution was incubated at 45ºC for 30 min. The lysate was homogenized by several passages through a sterile syringe and the final NaCl concentration was adjusted to 0.5 M. mRNA was purified by oligo(dT) cellulose binding (90 min at room temperature with gentle rotation). After several washing steps with binding[b] and low salt wash buffer[c] (to removes SDS and nonpolyadenylated RNAs), mRNA was eluted[d] and precipitated by adding 10 µl of 2

mg/ml glycogen carrier, 30 µl of 2 M sodium acetate and 600 µl of 100% ethanol (incubation overnight at -80°C). Finally, the sample was centrifuged at high speed (16000 x g, 15 min, 4°C) and the pellet containing mRNA was dried under heat lamp for 30 min to remove traces of ethanol. Reverse transcription of mRNA was performed using Advantage RT-for-PCR kit (Clontech). The pellet of mRNA was reconstituted in 12.5 µl of DEPC-treated H_2O and 1 µl of 20 µM oligo(dT) primer was added. First, the mix was heated at 70°C for 2 min and rapidly transferred on ice to remove RNA secondary structure. Then, the reverse transcription was initiated by adding to the sample 4 µl of 5X reaction buffer[e], 1 µl of dNTP mix (10 mM each), 0.5 µl of Recombinant RNase inhibitor (40 units/µl) and 1 µl of MMLV reverse transcriptase (200 units/µl), followed by incubation at 42°C (Mastercycler, Eppendorf). After 1 h, the reaction was stopped by incubation 5 min at 94ºC. Finally, the sample was diluted with DEPC-treated H_2O to obtain 100 µl of cDNA and stored at -20°C until PCR.

[a]***Lysis buffer***: *200 mM NaCl; 200 mM Tris-HCl, pH 7.5 ; 1.5 mM $MgCl_2$; 2 % SDS*
[b]***Binding buffer***: *500 mM NaCl; 10 mM Tris-HCl, pH 7.5 in DEPC-treated H_2O*
[c]***Low salt wash buffer***: *250 mM NaCl; 10 mM Tris-HCl, pH 7.5 in DEPC-treated H_2O*
[d]***Elution buffer***: *10 mM Tris-HCl, pH 7.5 in DEPC-treated H_2O*
[e]*5**X reaction buffer**: 250 mM Tris-HCl, pH 7.5; 375 mM KCl; 15 mM $MgCl_2$*

PCR

PCR was performed using specific primers designed in the conserved 5'- and 3'-UTR of cDNAs encoding AMP precursors of the dermaseptin superfamily (figure 13).

Forward primer 1: 5'-TGACCTTCAGTACCCAGCACTTTC-3' (24 bp, Tm: 56.3°C)
Reverse primer 1: 5'- GCATTTAGCTAAATGATATTCCACATCA-3' (28 bp, Tm: 56.2°C)

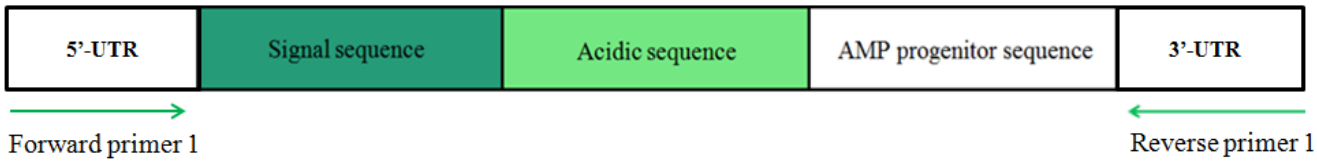

Figure 13: Position of the specific primers used for amplification of AMP cDNA precursors.

The following components were added in a tube:

- 25 µl of GoTaq Green Master Mix*, 2X (Promega)
- 18 µl of H_2O
- 1 µl of forward primer
- 1 µl of reverse primer
- 5 µl of cDNA

*__GoTaq Green Master Mix, 2X__: *DNA polymerase; reaction buffer, pH 8.5; 400 µM dATP; 400 µM dGTP; 400 µM dCTP; 400 µM dTTP; 3 mM* $MgCl_2$

PCR was done under the following conditions:

94 °C, 2 min – Initial denaturation

30 cycles {
- 94 °C, 45 s – Denaturation
- 55 °C, 1 min – Annealing
- 72 °C, 3 min – Extension

72 °C, 10 min – Final extension

After amplification, PCR products were analyzed by 1% agarose gel electrophoresis in the presence of GelRed (1:10000) (FluoProbes, Interchim). PCR fragments of interest corresponding to approximately 150-450 bp were then extracted and purified (Nucleospin Extract II kit, Macherey-Nagel) according to the manufacturer's protocol.

Cloning of PCR products into pGEM-T Easy vector

PCR products were cloned into pGEM-T Easy vector (pGEM-T Easy Vector Systems II, Promega), a plasmid that contain an ampicillin resistance gene as well as a β-galactosidase gene (*lac*Z) where fragment is cloned (figure 14). Ligation of the PCR product was performed by incubating all the components indicated in Table 6 at room temperature. A control insert DNA provided in the kit was used as positive control. The samples were incubated at 4°C during the weekend in order to increase the number of transformants.

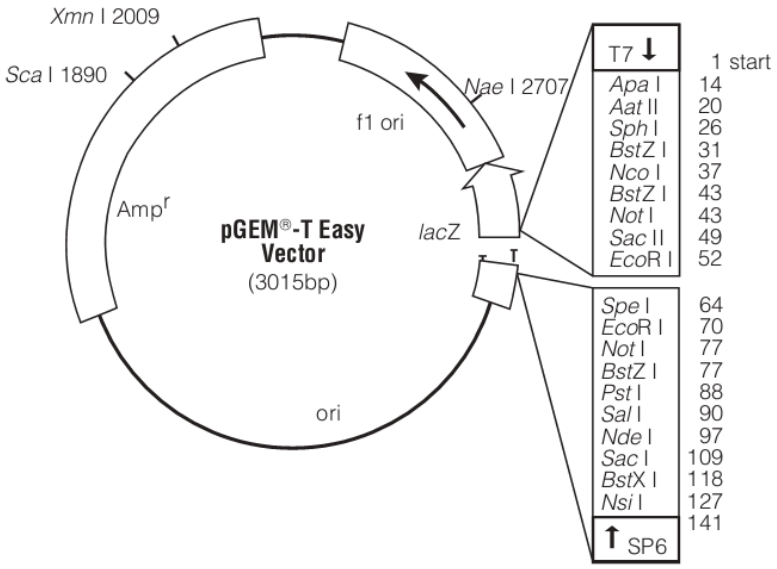

Figure 14: pGEM-T Easy Vector circle map.

Table 6: Ligation reaction of a PCR product into pGEM-T Easy vector. A control insert DNA was used as positive control.

	Standard Reaction	Positive Control
2X Rapid ligation buffer, T4 DNA ligase*	5 µl	5 µl
pGEM-T Easy vector (50 ng/µl)	1 µl	1 µl
PCR product	3 µl	-
Control insert DNA (4 ng/µl)	-	2 µl
T4 DNA ligase (3 Weiss units/µl)	1 µl	1 µl
Deionized water	-	1 µl

**2X Rapid ligation buffer, T4 DNA ligase : 60 mM Tris-HCl, pH 7.8 ; 20 mM $MgCl_2$; 20 mM DTT ; 2 mM ATP ; 10 % polyehylene glycol*

After ligation, *E. coli* bacteria (JM109 strain) were used for plasmid amplification. 2 µl of each ligation mixture were added to 50 µl of JM109 High Efficiency Competent Cells previously thawed on ice. The tubes were gently flicked and incubated on ice for 20 minutes. Then, the cells were heat-shocked for 45-50 seconds in a water bath at 42°C and immediately returned to ice for 2 minutes. After dilution with SOC medium, bacteria were allowed to grow (90 min at 37ºC with

shaking at 250 rpm) and were then spread on LB agar/ampicillin (100 mg/ml) Petri dishes containing IPTG (0.1 M) and X-gal (50 mg/ml) for blue/white screening. Plates were incubated overnight at 37ºC and bacteria containing recombinant plasmids (white colonies) were cultured in 5 ml of LB/ampicillin (100 mg/ml) overnight at 37 °C with shacking (250 rpm).

Plasmid DNA purification and determination of the insert size

Plasmid DNA purification was performed by Nucleospin Plasmid kit (Macherey-Nagel). Briefly, bacterial cultures were centrifuged (3000 rpm, 15 min, 4°C). The pellet was resuspended in an appropriate buffer* and plasmid DNA was liberated from *E. coli* host cells by SDS/alkaline lysis. After neutralization of lysate, precipitated protein, genomic DNA and cells debris were pelleted by centrifugation (11000 x g, 10 min), and supernatant was loaded onto a silica column that retains specifically plasmid DNA. Contaminants (salts, metabolites and soluble macromolecular cellular components) were removed by a washing step with an ethanolic buffer* and centrifugation (11000 x g, 1 min). After drying the silica membrane, pure plasmid DNA was eluted by centrifugation (11000 x g, 2 min) under low ionic strength conditions with 50 µl of 5 mM Tris-HCl, pH 8.5.

**The buffer composition was not provided by the supplier.*

As it can be seen in figure 14, pGEM-T Easy vector is flanked by two recognition sites for the restriction enzyme *Eco*R I. So, digestion of pure plasmid DNA by this restriction enzyme was performed to release the insert and determine its size. The following components were added in a tube and incubated for 90 min at 37°C:

- 5 µl of plasmid DNA
- 1 µl of 10X *Eco*R I buffer (900 mM Tris-HCl, pH 7.5; 100 mM $MgCl_2$; 500 mM NaCl, Promega)
- 0.5 µl of *Eco*R I enzyme (12 units/µl, Promega)
- 3.5 µl of Milli-Q H_2O

After digestion, 5 µl of this mix was analyzed by 1% agarose gel electrophoresis in the presence of GelRed (1:10000) and insert size were estimated using 100 bp DNA ladder (Promega). Plasmids containing inserts of the appropriate size (between 150 and 450 bp) were sequenced using T7 primer (Cogenics, Beckman Coulter Genomics, France).

9. Structural and functional characterization of temporin-SHe

Solid phase peptide synthesis

Temporin-SHe was synthesized by solid phase method using standard FastMoc chemistry (Applied Biosystems 433A automated peptide synthesizer - Peptide synthesis platform of IFR83, UPMC). Briefly, amino acids with α-NH_2 and side-chain protecting groups were added sequentially on a Rink amide PEG MBHA[a] resin from the C-terminus to the N-terminus (see figure 15 for the principle of peptide synthesis). Fmoc[b] protecting group were removed from α-NH_2 by addition of 20% piperidine/NMP[c] (deprotection step) and the activation of the carboxyl group was obtained with 0.5 M HBTU[d]/0.5 M HOBt[e]/DMF[f] and 2 M DIEA[g]/NMP (figure 15). At the end of synthesis, the N-terminus of the peptide was deprotected with piperidine and a scavenger mixture (95% TFA/2.5% TIS[h]/2.5% H_2O) was used to release peptide from the resin and remove protecting groups. Finally, after precipitation of the peptide with ether and several washing steps, the peptide was resuspended in 10% acetic acid and lyophilized. The crude synthetic temporin-SHe was purified by RP-HPLC on a semi-preparative column (Phenomenex Luna C18, 10 µm, 250 × 10 mm) with a 40-80% linear gradient of solvent B (1%/min) at a flow rate of 5 ml/min. The homogeneity and identity of temporin-SHe was confirmed by MALDI-TOF mass spectrometer (Voyager DE-Pro, Applied Byosystems) and analytical RP-HPLC on an Uptisphere C18 column (modulo-cart QS, 5 µm, ODS2, 250 x 4.6 mm, Interchim) using the conditions above with a flow rate of 0.75 ml.

[a] ***PEG MBHA:*** *Polyethylene glycol 4-methylbenzhydrylamine*
[b] ***Fmoc:*** *9-fluorenylmethoxycarbonyl*
[c] ***NMP:*** *N-methylpyrrolidone*
[d] ***HBTU****: O-Benzotriazole-N,N,N',N'-tetramethyl-uronium-hexafluoro-phosphate*
[e] ***HOBt****: N-Hydroxybenzotriazole*
[f] ***DMF****: Dimethylformamide*
[g] ***DIEA****: N,N-Diisopropylethylamine*
[h] ***TIS:*** *(triisopropylsilane)*

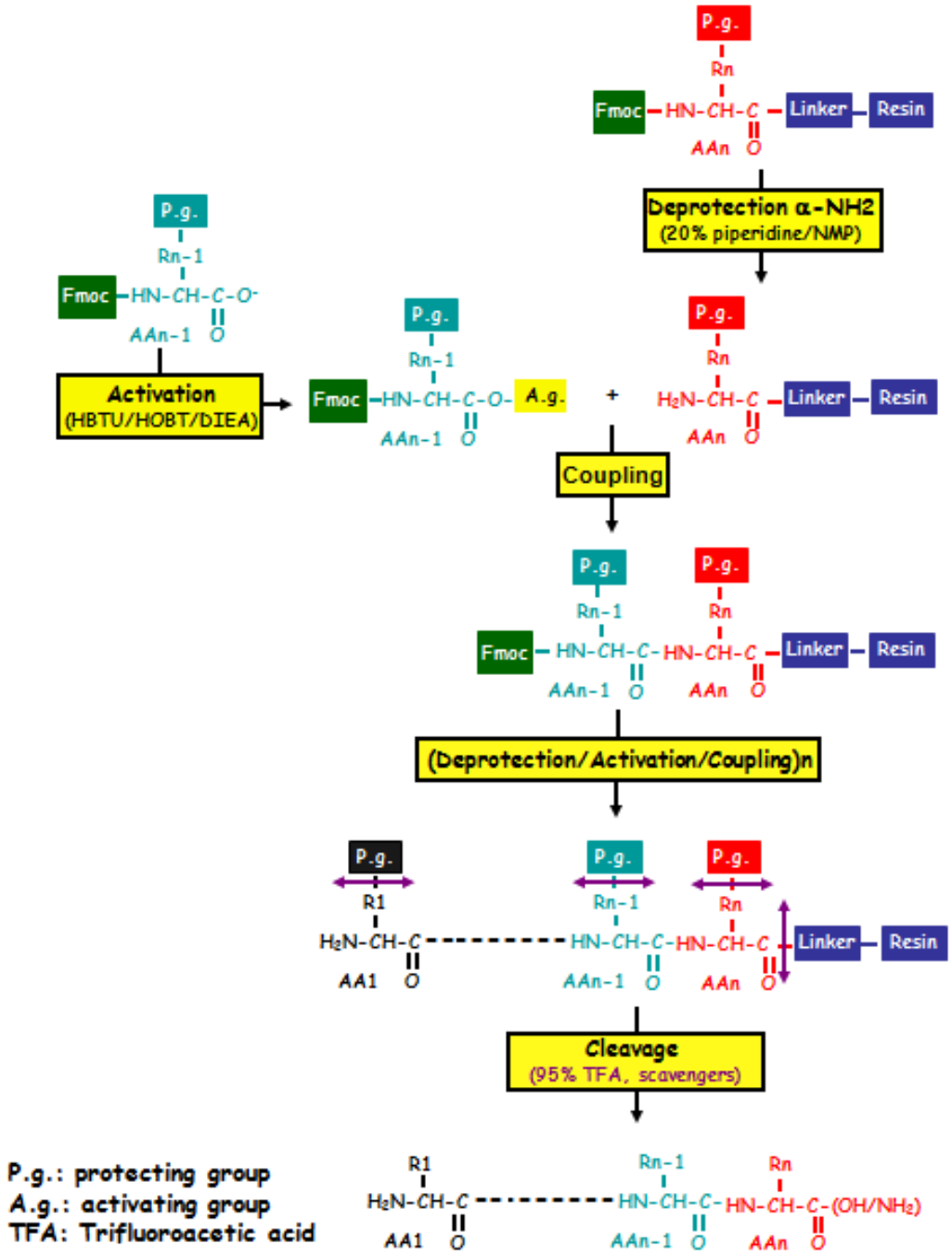

Figure 15: Schematic representation of solid phase peptide synthesis using FastMoc chemistry. The first step corresponds to the deprotection of the α-NH_2 group of the first amino acid attached to the resin (i.e. AA_n, corresponding to the C-terminal residue of the peptide). Then, the α-COOH group of the next amino acid (AA_{n-1}) is activated in order to form a peptide bond with the deprotected amino acid (AA_n) after coupling. Deprotection/activation/coupling steps are repeated until the peptide chain is complete. Finally, after depotection of the N-terminus, the side-chain protecting groups are removed and the peptide is cleaved from the resin. Fmoc: 9-fluorenylmethoxycarbonyl; NMP: N-methylpyrrolidone; HBTU: O-Benzotriazole-N,N,N',N'-tetramethyl-uronium-hexafluoro-phosphate; HOBt: N-Hydroxybenzotriazole; DIEA: N,N-Diisopropylethylamine.

Preparation of multilamellar and large unilamellar vesicles

DMPC (dimyristoyl phosphatidyl choline) and DMPG (dimyristoyl phosphatidyl glycerol) were purchased from Avanti Polar lipids. DMPC (1.5 mg) was dissolved in 150 µl of chloroform and a mix of DMPC/DMPG 3:1 (mol/mol) (i.e. 1.12 mg of DMPC and 0.38 mg of DMPG) was also prepared and dissolved in chloroform/methanol (1:1). The samples were then dried under a nitrogen stream, and lipid films were kept under vacuum for 3h at 45°C to remove all traces of organic solvents. Multilamellar vesicles (MLVs) were obtained by hydrating the dry lipid films with 1.5 ml of PBS buffer (10 mM Na_2HPO_4, 100 mM NaCl, pH 7.3) at 37°C (10°C above the lipid phase transition) and vortexing until a homogeneous suspension was formed (1 mg of MLVs/ml). MLVs were used for differential scanning calorimetry experiments. For circular dichroism experiments, large unilamellar vesicles (LUVs) were obtained from dry lipid films by hydration with 1.5 ml of phosphate buffer (10 mM Na_2HPO_4, pH 7.3), followed by seven rounds of freeze-thawing (liquid nitrogen/water bath at 37°C) and extrusion through different polycarbonate membranes (400, 200 and 100 nm pore size).

Circular dichroism spectroscopy

The secondary structure of temporin-SHe was determined by circular dichroism (CD) spectroscopy using zwitterionic DMPC LUVs (eukaryote membrane model) or negatively charged DMPC/DMPG (3:1) LUVs (bacterial membrane model). CD spectra were recorded at 25°C with a Jobin Yvon CD6 spectropolarimeter in a 0.1-cm quartz cell over a wavelength range from 185 to 260 nm. Spectra were acquired with a spectral bandwidth of 2-nm, a step size of 0.5 nm and a time constant of 3.0 s. Experiments were done with different temporin-SHe/lipid molar ratios (1:200, 1:100 and 1:50) and also with peptide (30 µM) in phosphate buffer (10 mM Na_2HPO_4, pH 7.3) or 80 mM SDS. The baselines (DMPC, DMPC/DMPG 3:1, phosphate buffer and 80 mM SDS) were acquired independently under the same conditions and then subtracted from the corresponding peptide spectra. CD measurements were reported as $\Delta\varepsilon$ (M^{-1}. cm^{-1}) per residue. $\Delta\varepsilon$: dichroic increment.

Analysis of peptide-lipid interaction by differential scanning calorimetry

The interaction of synthetic temporin-SHe with membrane vesicles (MLVs) was analyzed by differential scanning calorimetry (DSC). DMPC/DMPG 3:1 was used as a model system for bacterial membranes. Different peptide/lipid molar ratios (1:200, 1:100 and 1:50) were used. Calorimetry experiments were performed with a Nano III calorimeter (Calorimetry Sciences Corp., USA) using a temperature range of 0-35°C with heating and cooling rates of 0.5°C/min and 1.5°C/min, respectively. Several scans (>20) were run for each sample with a 10 min equilibration time between each scan. The raw data were analyzed with the CpCalc software. Thermograms corresponding to the heating scans were converted to molar heat capacity (ΔCp) using average lipid molecular weight, partial specific volume (0.73 ml/g), peptide concentration and cell volume (299 µl), and the value of the transition temperature was estimated.

Biological membranes can adopt different physical states, i.e., from a gel phase (Lβ') to a liquid crystalline phase (Lα) with an intermediate rippled gel phase (Pβ') (figure 16) (reviewed in [80]). The transition from one phase to another requires a specific temperature that can be measured by DSC to analyze the interaction of the peptide with the membrane and also its degree of insertion into the lipid bilayer.

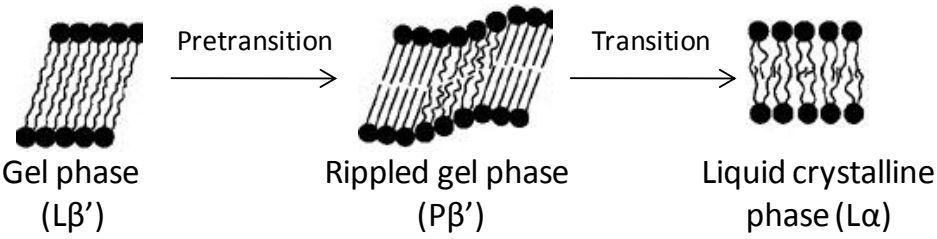

Figure 16: Scheme illustrating the different physical states adopted by a lipid bilayer. The pretransition corresponds to the conversion of the ordered lamellar gel phase (Lβ'), with tilted hydrocarbon chains, to the rippled gel phase (Pβ'). The main transition corresponds to the conversion of the rippled gel phase (Pβ') to the fluid lamellar liquid crystalline phase (Lα).

Permeabilization assay

The ability of temporin-SHe to permeabilize the cytoplasmic membrane of Gram-positive (*S. aureus* ST1065) and Gram-negative (*E. coli* ML-35p) bacteria was determined. *E. coli* ML-35p and *S. aureus* ST1065 were kindly provided by Prof. Sylvie Rebuffat (National Museum of Natural History, MNHN, Paris, France) and Dr. Tarek Msadek (Institut Pasteur, Paris, France), respectively. These bacterial strains express constitutively cytoplasmic β-galactosidase. *E. coli* ML-35p is ampicillin resistant and lactose permease deficient, whereas *S. aureus* ST1065 is only chloramphenicol resistant. If the peptide permeates the bacterial inner membrane, the chromogenic substrate ONPG (ortho-nitrophenyl-β-D-galactopyranoside, Sigma) can enter the cytoplasm and be hydrolyzed into ONP (ortho-nitrophenol) by cytoplasmic β-galactosidase. So, the permeabilization of the bacterial membrane can be measured by monitoring ONP production at 405 nm. Briefly, strains were cultured in LB medium for 2-3 h at 37°C with shaking (250 rpm), centrifuged (1000 x g, 10 min, 4°C) washed three times with sterile PBS buffer (10 mM Na_2HPO_4, 100 mM NaCl, pH 7.3) and resuspended in the same buffer to obtain A_{600} = 0.05. The assay was performed in sterilized 96-well plates in a final volume of 150 µl: 15 µl of the bacterial suspension were added to 135 µl of PBS buffer supplemented with 2.5 mM ONPG and containing the peptide at different concentrations (at MIC, below and above the MIC). Hydrolysis of ONPG was monitored by measuring absorbance at 405 nm every 5 min during 120 min at 37°C (Fluostar Galaxy, BMG Labtech). PBS buffer with 2.5 mM ONPG but without peptide was used as negative control, and temporin-SHx (10 µM), a potent synthetic temporin analogue, was used as positive control. Three independent experiments were performed in quadruplicate. Results were expressed as the mean ± S.E.M. of a representative experiment.

Time killing assay

To study the bactericidal effect and the rate of killing of temporin-SHe, the peptide was added to a bacterial suspension of *E. coli* ATCC 25922 or *S. aureus* ST1065 and the number of viable bacteria was determined at 37°C according to the time. Bacteria were cultured in LB medium for 2-3 h at 37°C with shaking (250 rpm), centrifuged (1000 x g, 10 min, 4°C), washed three times with sterile PBS buffer (10 mM Na_2HPO_4, 100 mM NaCl, pH 7.3) and resuspended in the same buffer to obtain approximately 10^6 cfu/ml. 100 µl of temporin-SHe at a final concentration two-fold above the MIC (50 µM for *E. coli* ATCC 25922 and 6.25 µM for *S. aureus* ST1065) were mixed with 100 µl of the bacterial suspension (10^6 cfu/ml). At each time (0, 5, 15, 30, 45, 60, 90 and 120 min), 10 µl of the mixture was withdrawn and diluted 40000-fold in LB medium and spread on LB agar plates for cell counting after overnight incubation at 37ºC. Control was run without peptide (100 µl of PBS buffer). Three independent experiments were performed in triplicate. Results were expressed as the mean ± S.E.M. of a representative experiment.

RESULTS

Analysis of skin secretions of *T. resinifictrix*

126 mg of lyophilized skin secretions were obtained from four adult specimens of *T. resinifictrix* by electrical stimulation. The lyophilisate was pre-purified on a Sep-Pak C18 cartridge and then chromatographed on a semi-preparative RP-HPLC C18 column (figure 17). The eluted material was fractionated into tubes at 1 min per tube (i.e. fractions of 4 ml). Tubes of four series injection (1.5 ml per injection) corresponding to the same time were pooled and lyophilized in order to concentrate the peptidic material. Fractions were reconstituted in sterile H_2O and tested for their ability to inhibit growth of the Gram-positive reference strain *S. aureus*. As shown in figure 18, several fractions inhibited strongly the growth of *S. aureus*. A complete inhibition was observed for fraction 37, and about 90% inhibition for fractions 25 and 29. Other fractions (5, 30 and 31) were also able to inhibit bacterial growth, although to a lesser extent (around 50%). By contrast, stimulation was observed for several fractions, particularly for fractions 15-22 displaying potent stimulation ($\geq$ 200%).

Fractions with high inhibitory activity (i.e. 25, 29 and 37) were rechromatographed on an analytical RP-HPLC C18 column using a slower gradient of ACN (0.5%/min) to improve peaks separation (figure 19). Regions corresponding to peaks in the different fractions were collected manually (figure 19) and then tested against *S. aureus*. Only peak 6 of fraction 25 (figure 19 A) showed a potent bacterial growth inhibition (figure 20). The material present in this peak was subjected to MALDI-TOF mass spectrometry. As shown in figure 21, several ionic species with monoisotopic masses ($[M+H]^+$) ranging from approximately 1000 to 1900 Da (1051.46, 1165.36, 1334.32, 1448.22, 1822.81 Da) were observed and could thus correspond to AMPs of 10-17 residues long. We attempted to determine their primary structure by tandem mass spectrometry (MS/MS) in collaboration with Prof. Edwin De Pauw (Mass Spectrometry Laboratory, University of Liège, Belgium). Unfortunately, due to insufficient material in the sample, we were unable to obtain sequence information.

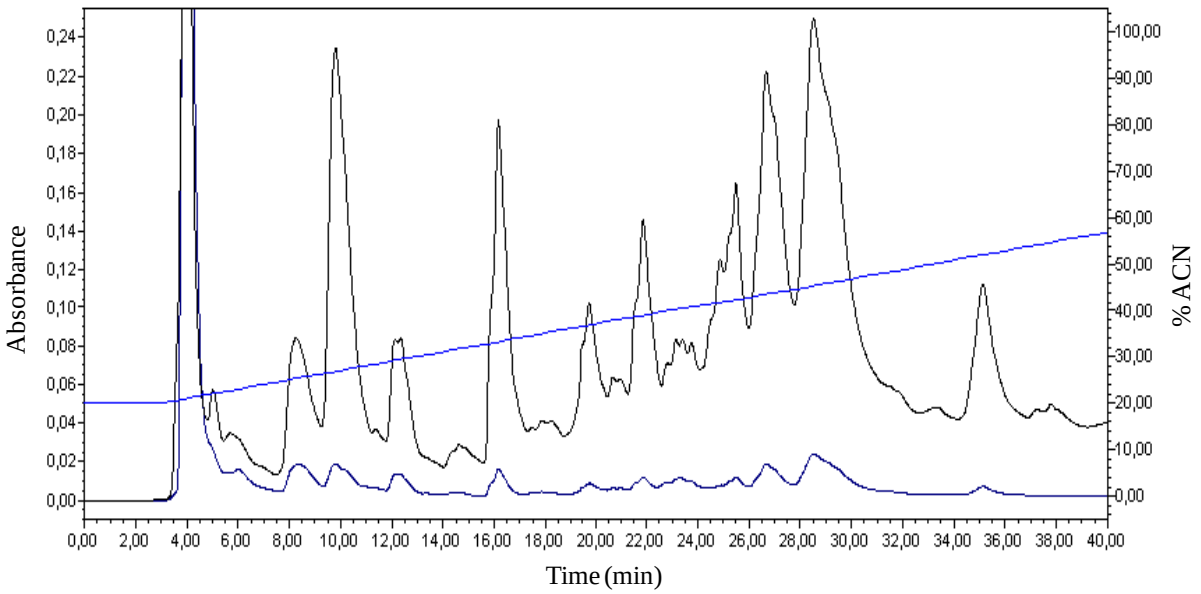

Figure 17: RP-HPLC chromatogram of skin secretions of *T. resinifictrix*. After pre-purification on a Sep-Pak C18 cartridge, skin secretions were fractionated on a semi-preparative Nucleosil C18 column (5 µm, 250 x 10 mm, Interchim) using a 20-60% linear gradient of ACN (1%/min) (blue line) at a flow rate of 4 ml/min. Fractions were collected each minute and absorbance was monitored at 220 (dark) and 280 nm (blue).

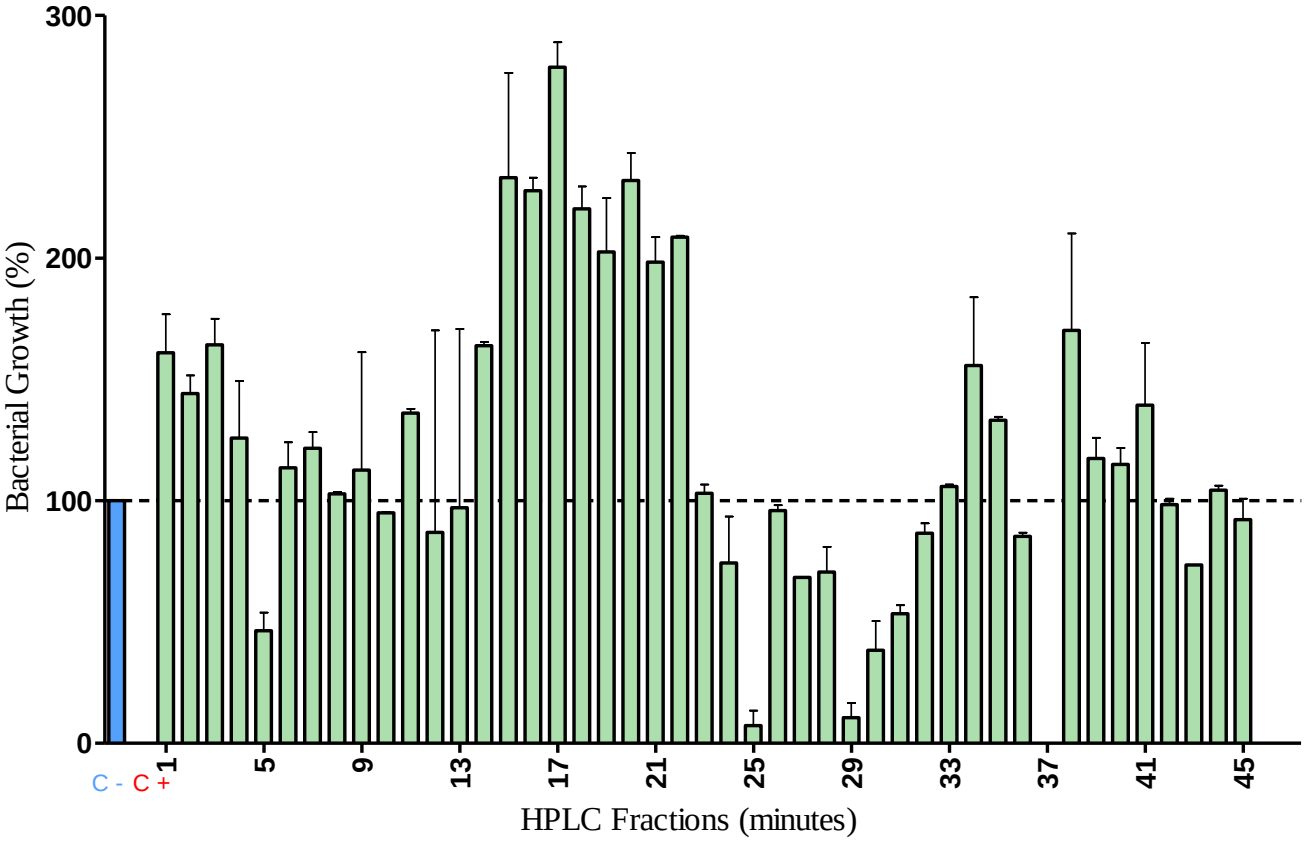

Figure 18: Antibacterial activity (*S. aureus*) of semi-preparative HPLC fractions. Measures were realized in duplicate and represent the mean ± S.E.M. Results are expressed as percent of bacterial growth using H_2O (100% growth, C-) and 0.7% formaldehyde (0% growth, C+) as controls.

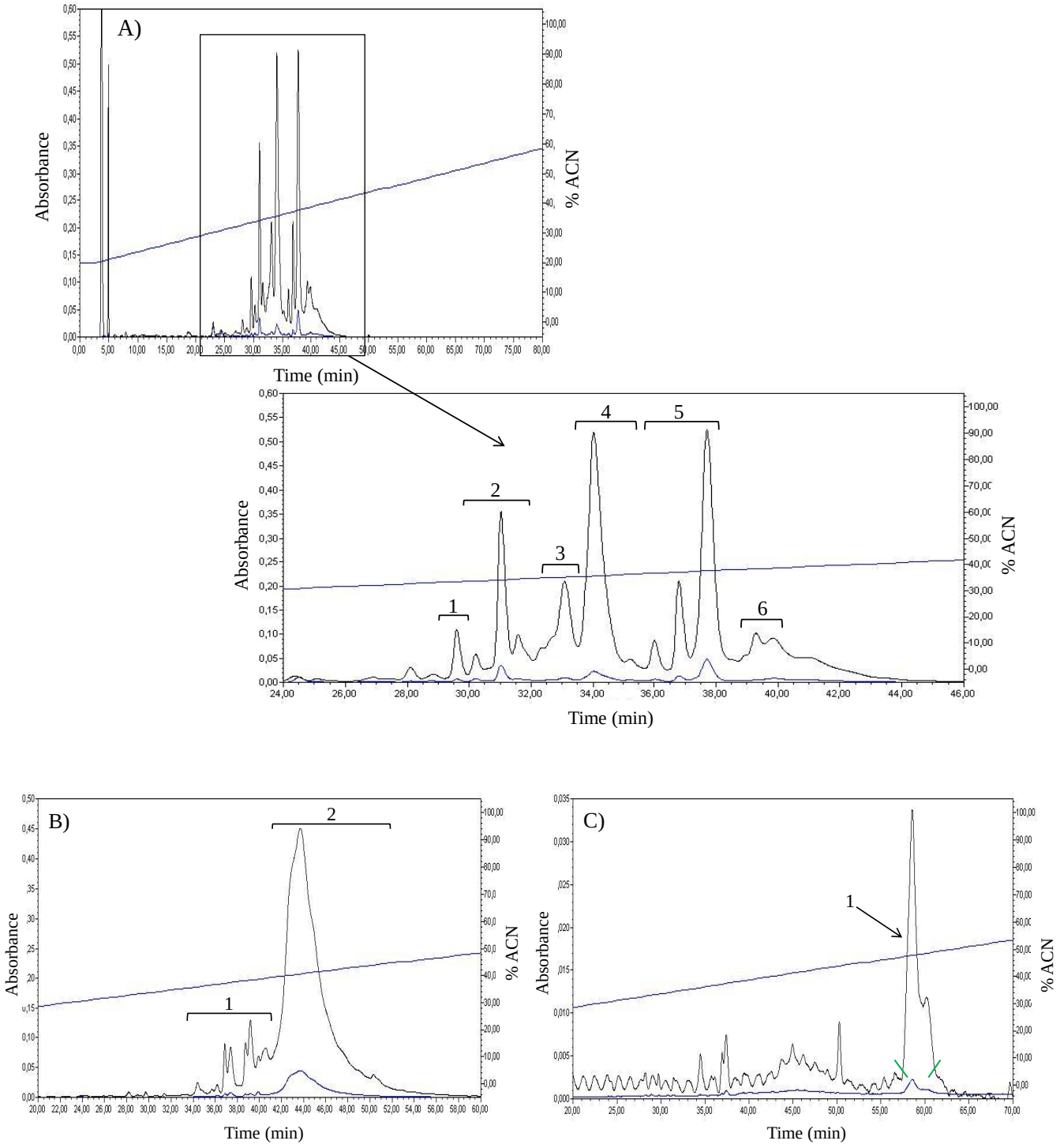

Figure 19: Analytical chromatograms of antibacterial fractions (25, 29 and 37). The material of the active semi-preparative fractions was rechromatographed on an Uptisphere C18 analytical column using a 20-60% linear gradient of ACN at a slower rate (0.5%/min) (blue line) and with a flow rate of 0.75 ml/min. A) Fraction 25 (a zoom of the region 24-46 min is shown), B) Fraction 29, C) Fraction 37. The manually collected regions of each fraction are indicated by a number. Absorbance was monitored at 220 (dark) and 280 nm (blue).

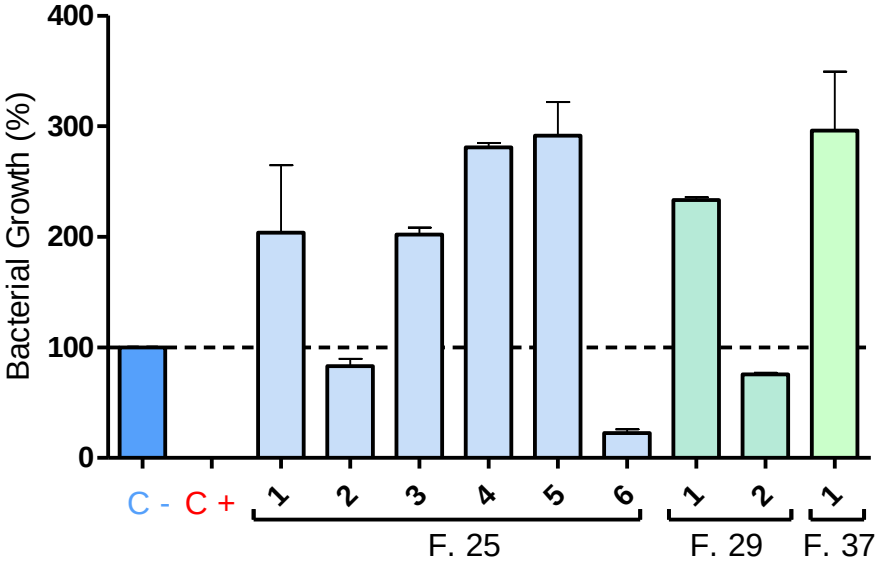

Figure 20: Antibacterial activity of the different peaks of fractions 25, 29 and 37. Each number corresponds to peaks harvested manually (see figure 19). Measures were realized in duplicate and represent the mean ± S.E.M. Results are expressed as percent of bacterial growth using H_2O (100% growth, C-) and 0.7% formaldehyde (0% growth, C+) as controls.

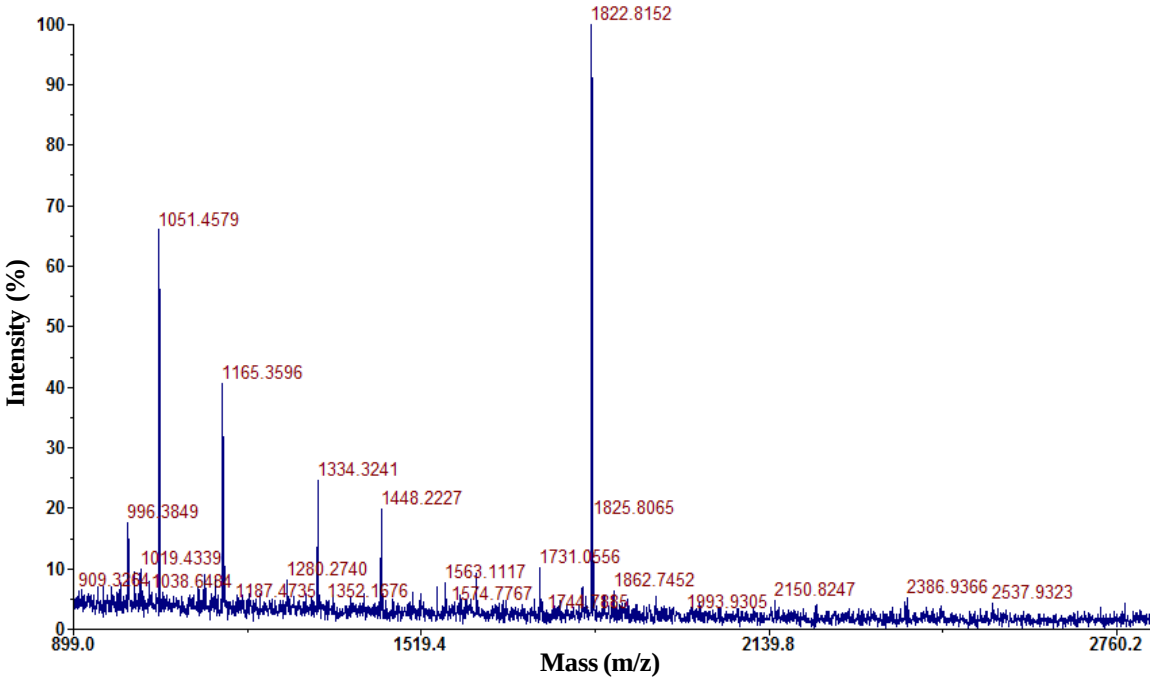

Figure 21: MALDI-TOF mass spectrum of peak 6 (fraction 25)

cDNA cloning of AMP precursors from skin secretions of *T. resinifictrix*

Poly(A)$^+$ RNA was extracted from about 17 mg of skin secretions of *T. resinifictrix* and converted into cDNA by RT-PCR using an oligo(dT) primer. A PCR was then realized using specific oligonucleotides (forward primer 1/reverse primer 1) designed to the conserved 5'- and 3'-UTR of cDNAs encoding AMP precursors of the dermaseptin superfamily. Since no band was observed after 1% agarose gel electrophoresis, we have performed a reamplification with the same primers (figure 22 A). After this second PCR, we observed the presence of different bands, and particularly of low intensity (≥ 200 bp) that could correspond to the size of AMP precursors (figure 22 A). So, PCR products were purified from the amplified solution and concentrated. After cloning into pGEM-T Easy vector and amplification in JM109 competent cells, plasmid purification was done from positive (white) colonies. Enzymatic digestion by *Eco*R I revealed clones with an insert size between 150 and 500 bp (figure 22 B). These clones (clones 1, 2, 3, 5, 6 and 8) were sequenced by Cogenics (Beckman Coulter Genomics, France) using the T7 primer, but unfortunately no insert corresponding to an AMP precursor was obtained after sequence analysis with DNA translator 1.1 and BLAST search.

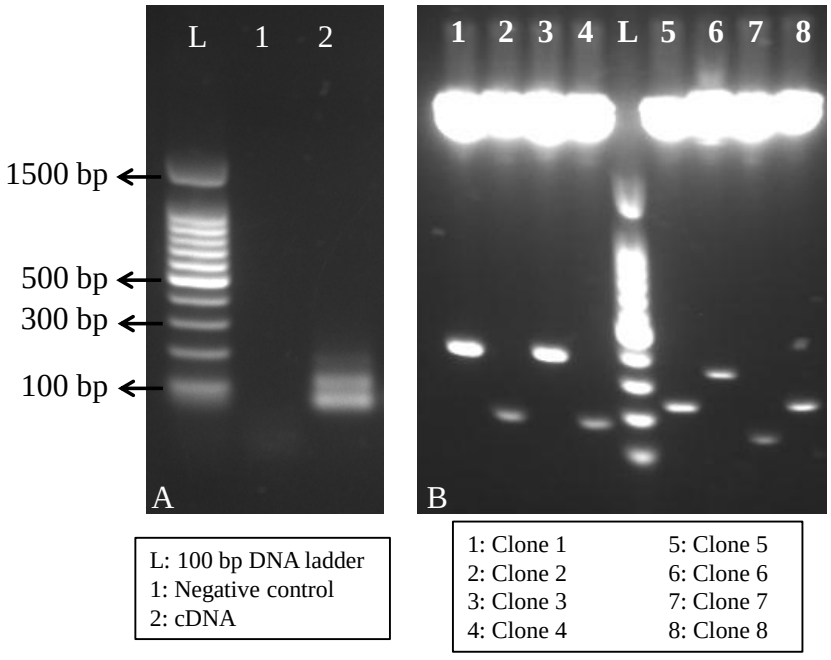

Figure 22: Analytical agarose gel electrophoresis after PCR (A) and enzymatic digestion (B). A) 5 µl of the first PCR was reamplified with the same primers (forward primer 1/reverse primer 1). Negative control was performed without DNA. B) Enzymatic digestion of plasmidic clones by *Eco*R I. L: 100 bp DNA ladder

During my training, several attempts were made to amplify AMP precursors. I have realized PCRs with different annealing temperatures and different sets of primers designed to other conserved regions (i.e. signal sequence and acidic proregion) of AMP precursors of the dermaseptin superfamily. However, after cloning of the PCR products, plasmid purification and sequence analysis, negative results were obtained.

Structural and functional characterization of temporin-SHe

The second aim of my Master 2 internship was to characterize the structure and function of temporin-SHe and also to compare this peptide to its paralog, temporin-SHd, an AMP already studied by Abbassi/Raja and co-workers [77]. Indeed, among all the identified temporins from *Pelophylax saharica* [72, 76], temporin-SHd shares the highest identity (76.5%) with temporin-SHe (figure 23). Moreover, the amino acid composition of these both peptides is quasi-identical with only an additional glycine residue for temporin-SHd.

```
Temporin_SHd      FLPAALAGIGGILGKLF
Temporin_SHe      FLP-ALAGIAGLLGKIF
Temporin_SHa      FL----SGIVGMLGKLF
Temporin_SHb      FLP----IVTNLLSGLL
Temporin_SHc      FLS----HIAGFLSNLF
Temporin_SHf      FF---------FLSRIF
```

	% Identity with temporin-SHe
Temporin-SHa	56.2
Temporin-SHb	35.3
Temporin-SHc	43.7
Temporin-SHd	76.5
Temporin-SHf	25.0

Figure 23: Alignment of the amino acid sequences of temporins-SH and percent identity. Alignment was realized with ClustalW multiple alignment. Percent identities were obtained from ClustalW pairwise alignment of temporins-SH with temporin-SHe. Identical and similar (strongly and weakly) residues are highlighted in blue and yellow, respectively.

Synthesis and purification of temporin-SHe

After solid phase synthesis and purification of the crude peptide by RP-HPLC, about 28 mg of lyophilized powder of temporin-SHe was obtained. In order to confirm the purity and integrity of the purified peptide, 10 µg was injected onto an analytical RP-HPLC C18 column with a 40-80% linear gradient of ACN (1%/min), and 10 pmol was also analyzed by MALDI-TOF mass spectrometry. For comparison, synthetic temporin-SHd was analyzed in the same conditions. As shown in figure 24, temporin-SHe is eluted at 31 min (i.e. 68% ACN), whereas temporin-SHd is eluted at approximately 24 min (61% ACN), indicating that the first one is more hydrophobic. A quasi-single homogeneous peak is observed for both peptides, revealing also high purity (> 95%). The little peak eluting at ~ 15 min, which is present in the two HPLC chromatograms, corresponds to the background noise of the column and was observed after injection of H_2O-0.1% TFA without peptide (data not shown). MALDI-TOF mass spectrum of temporin-SHe revealed the presence of cationic adducts ($[M+Na]^+$ = 1622.0 Da, $[M+K]^+$ = 1637.9 Da) with no $[M+H]^+$ ion (1599.99 Da) (figure 24). No additional compound was detected, thus confirming the purity and integrity of the synthetic temporin-SHe.

Secondary structure of temporin-SHe

To explore the secondary structure of temporin-SHe, we performed an extensive circular dichroism (CD) study of the peptide in different media: PBS buffer, DMPC or DMPC/DMPG 3:1 LUVs, SDS 80 mM (figure 25). As shown in figure 25 D, temporin-SHe exhibited a typical random coil signal in PBS buffer (minimum around 200 nm), indicating no ordered structure for this peptide in solution. By contrast, in membrane-mimetic environments such as SDS or LUVs (DMPC and DMPC/DMPG), temporin-SHe was structured in α-helix with characteristic minima at 208 and 222 nm (figure 25). However, in the presence of zwitterionic DMPC LUVs (1:200 and 1:100) or SDS, a difference in the intensity of these two minima was observed with a more pronounced minimum at 208 nm (figure 25 A, B and D). This suggests the presence of a mix structure, i.e. random coil and α-helix conformations.

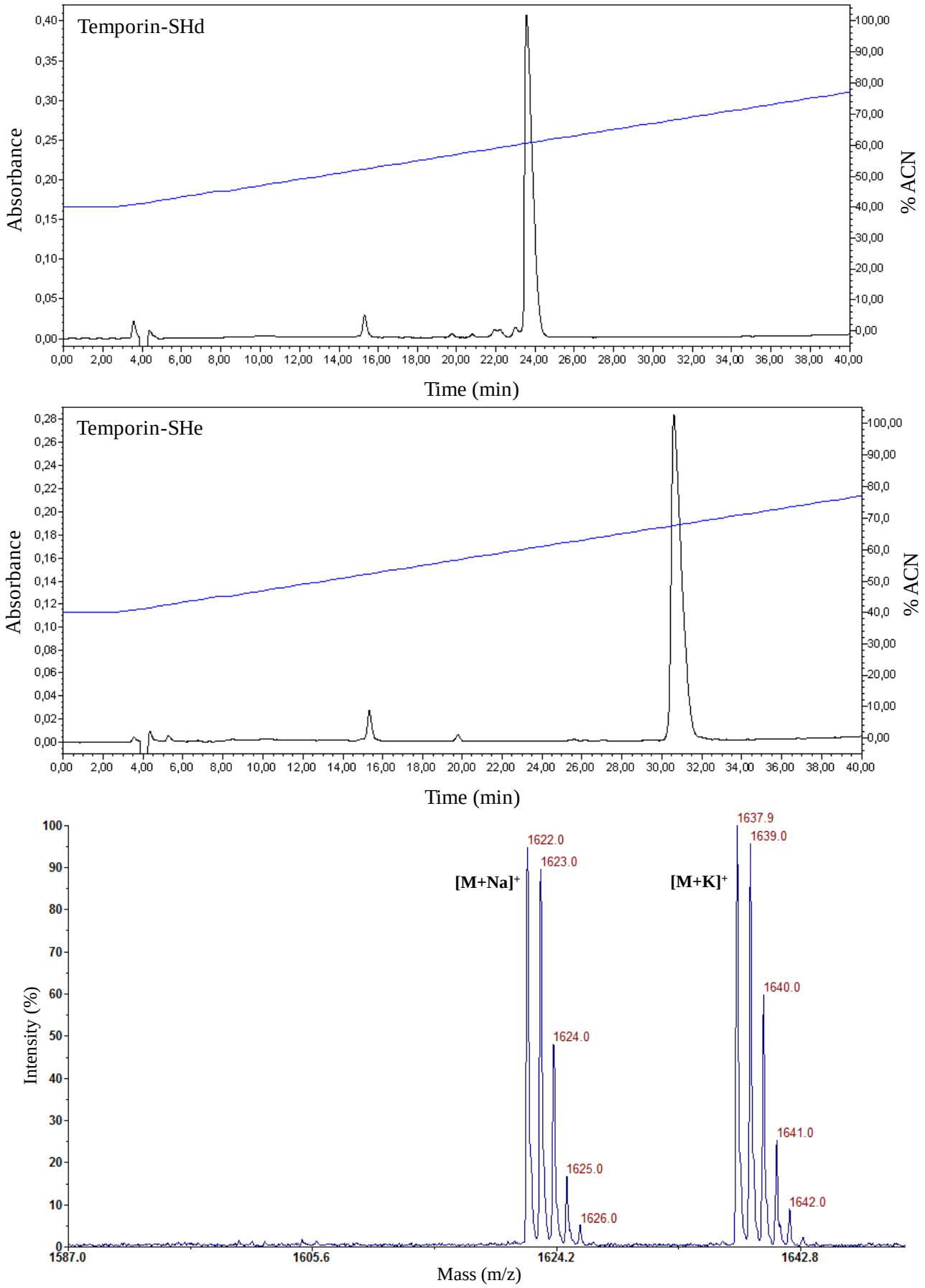

Figure 24: Analytical RP-HPLC chromatograms and mass spectrum of synthetic temporin-SHe. Peptides were analyzed on a C18 column (Uptisphere) using a 40-80% linear gradient of ACN (1%/min) (blue line) at a flow rate of 0.75 ml/min. Absorbance was monitored at 220 nm. For the MS spectrum, the cluster of peaks corresponding to isotopic variants of $[M + Na]^+$ and $[M + K]^+$ ions are indicated

With DMPC/DMPG LUVs (figure 25 A, B and C) or when the peptide concentration was increased for DMPC (DMPC 1:50, figure 25 C), we noticed a well-defined α-helical conformation with two minima (208 and 222 nm) of approximately the same intensity. This clearly indicates that negatively charged membranes compared to zwitterionic membranes promote a better α-helical structuration of temporin-SHe. This phenomenon was also observed for temporin-SHd [77]. No amphipathic character, with two well-separated polar and apolar faces, is observed when the sequence of temporin-SHe and -SHd is plotted on a Schiffer-Edmundson helical wheel (figure 26).

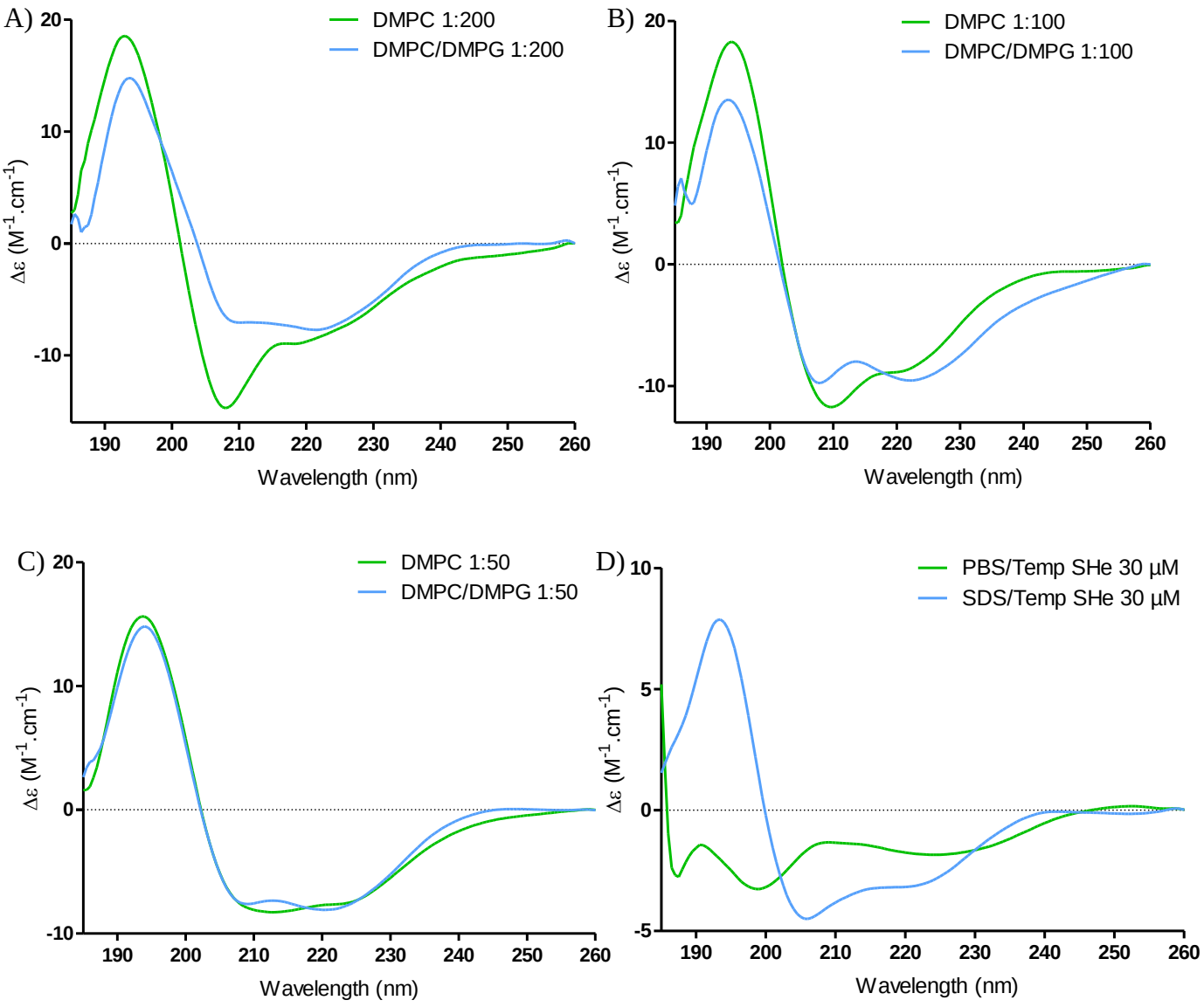

Figure 25: α-helix structure of temporin-SHe in membrane mimicking environment (DMPC and DMPC/DMPG 3:1 LUVs). Different peptide/lipid molar ratios were tested: 1:200 (A), 1:100 (B) and 1:50 (C). CD spectra of 30 µM temporin-SHe were also obtained in 10 mM PBS (unordered structure) and 80 mM SDS (D).

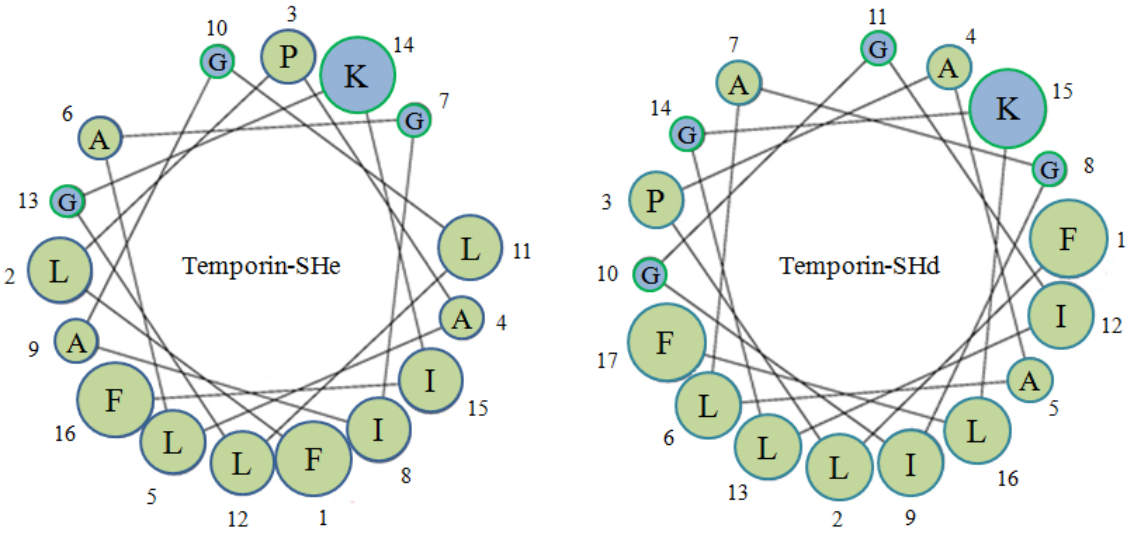

Figure 26: Schiffer-Edmundson helical wheel diagram of temporin-SHe and -SHd. Residues are represented proportional to amino acid volume. Apolar residues are represented in green and polar residues in blue. No amphipathic character, with two well-separated polar and apolar faces, is observed.

Interaction of temporin-SHe with anionic model membranes

Differential scanning calorimetry (DSC) technique was used to study the thermotropic behavior of DMPC/DMPG multilamellar vesicles (MLVs) upon addition of temporin-SHe. Negatively charged DMPC/DMPG (3:1) MLVs were chosen as a model for bacterial membranes. These MLVs exhibit two endothermic events on heating, a weakly energetic pretransition near 13°C (conversion of the ordered gel phase, Lβ', to the rippled gel phase, Pβ') and a strongly energetic main transition near 24°C (conversion of the rippled gel phase to the liquid-crystalline phase, Lα) (Figure 27). The pretransition is due to interactions between the phospholipid headgroups, and increasing the distance between them causes the pretransition peak to disappear **(**reviewed in [76]). We observed that the pretransition peak was reduced (peptide-lipid ratio 1:200) or abolished (ratios 1:100 and 1:50) in the presence of temporin-SHe (figure 27), indicating electrostatic interactions between the cationic peptide and the anionic lipid headgroups. The main phase transition is mainly due to *trans-gauche* interconversion of the acyl chains, which decreases the acyl chain packing and increases fluidity of the membrane (reviewed in [76, 81]). As shown in figure 27, increasing concentrations of temporin-SHe induced a two-component main phase transition (peptide-lipid ratio 1:50) consisting of a broad higher temperature and less cooperative component superimposed over a sharper lower temperature component. This indicates

that the peptide affects hydrocarbon chain packing, disturbing strongly the membrane bilayer, with the occurrence of peptide-poor (sharp component) and peptide-rich (broad component) phospholipid domains [78, 81].

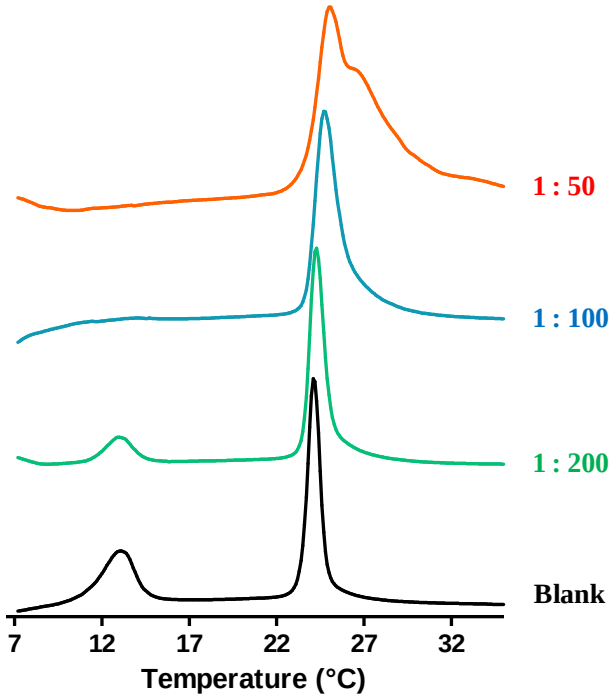

Figure 27: DSC heating thermograms illustrating the effect of temporin-SHe on the thermotropic phase behavior of DMPC/DMPG (3:1) MLVs. Scans were acquired without peptide (blank) and at different peptide/lipid molar ratios (1:200, 1:100 and 1:50).

Antimicrobial and cytotoxic activities of temporin-SHe

The antimicrobial activity of synthetic temporin-SHe was assayed against various microorganisms, including bacteria, yeasts and protozoa. As shown in Table 7, temporin-SHe has a broad-spectrum activity. This peptide displays high potency against Gram-positive bacteria and *S. cerevisiae* with two-fold higher activity (MIC = 1.5-12.5 µM) compared to temporin-SHd. For both temporins, the activities against antibiotic-multiresistant *S. aureus* strains (ATCC 43300 and ATCC BAA-44) were as potent as those against non-resistant strains (*S. aureus* ATCC 25923 and ST1065). Good activity was also observed toward the Gram-negative reference strain *E. coli* ATCC 25922 (MIC = 25 and 5 µM for temporin-SHe and -SHd, respectively). Other Gram-negative bacteria were sensitive to temporin-SHe, such as the naturally more resistant strain

Pseudomonas aeruginosa (MIC = 60 µM) or the fungus *Candida parapsilosis* (MIC = 50 µM), whereas they were resistant to temporin-SHd (MIC ≥ 200 µM).

Antiparasitic activity of temporin-SHe was also analyzed by Z. Raja, a PhD student of the team, in collaboration with Dr. B. Oury and Dr. D. Sereno (Research Institute for Development, Montpellier, France). As indicated in table 7, temporin-SHe kills efficiently *Leishmania* promastigotes (insect stage) with an activity (IC_{50} ~ 10 µM) in the same range as temporin-SHd. A preliminary study, also realized in Montpellier, was done to evaluate the cytotoxicity of temporins on mammalian cells (THP-1 monocytes). It was observed that temporin-SHe was three-fold more cytotoxic than temporin-SHd (Table 7).

Permeabilization of the bacterial cytoplasmic membrane

The ability of temporin-SHe to permeate the cytoplasmic membrane of the Gram-negative *E. coli* ML-35p and the Gram-positive *S. aureus* ST1065 was studied by monitoring the hydrolysis of the chromogenic extracellular substrate ONPG into ONP by bacterial cytoplasmic β-galactosidase. As shown in figure 28, temporin-SHe permeabilized the cytoplasmic membranes of both bacteria in a time- and concentration-dependent manner. However, *S. aureus* bacteria were permeabilized faster and to a higher extent than *E. coli*. Indeed, at concentrations above the MIC (> 3.1 µM), the efficiency of temporin-SHe was similar to temporin-SHx (10 µM), a potent temporin-SHa analog used as positive control (figure 28 B). Membrane permeability was observed even at concentration below the MIC. Our results are similar to those obtained for temporin-SHd by Abbassi/Raja and co-workers [77].

Table 7: Antimicrobial and cytotoxic activities of temporin-SHe. Minimal inhibitory concentration (MIC) is expressed as average values from three independent experiments performed in triplicate. Inhibitory concentration 50 (IC_{50}) values are also indicated. For comparison, activities of temporin-SHd were included in the table and were taken from reference [77].

	Temporin-SHe	Temporin-SHd
Gram-negative bacteria	MIC (µM)	
Escherichia coli ATCC 25922	25	5
E. coli ATCC 35218	50	50
E. coli ML-35p	50	25
Pseudomonas aeruginosa ATCC 27853	60	> 200
Gram-positive bacteria		
Staphylococcus aureus ATCC 25923	3.1	6.2
S. aureus ATCC 43300[a]	3.1	6.2
S. aureus ATCC BAA-44[b]	3.1	6.2
S. aureus ST1065	3.1	6.2
Enterococcus faecalis ATCC 29212	12.5	2
Bacillus megaterium	1.5	1.5
Listeria ivanovii	5	10
Yeasts		
Candida albicans ATCC 90028	> 100	100
C. parapsilosis ATCC 22019	50	> 200
Saccharomyces cerevisiae	12.5	25
Protozoa[c]	IC_{50} (µM)	
Leishmania infantum	14.0	19.0
L. major	10.5	14.5
L. braziliensis	10.5	18.0
THP-1 monocytes[d]	LC_{50} (µM)	
	21 µM	66 µM

[a] *Resistant to methicillin and oxacillin.*
[b] *Resistant to amoxicillin/clavulanic acid, cephalothin, ciprofloxacin, erythromycin, gentamicin, imipenem, oxacillin, penicillin, tetracycline, ampicillin, doxycycline, methicillin, azithromycin, ceftriaxone, clindamycin, lincomycin, perfloxacin, rifampin and tobramycin.*
[c] *Promastigote stage of the human parasite Leishmania*
[d] *Human acute monocytic leukemia cell line.*

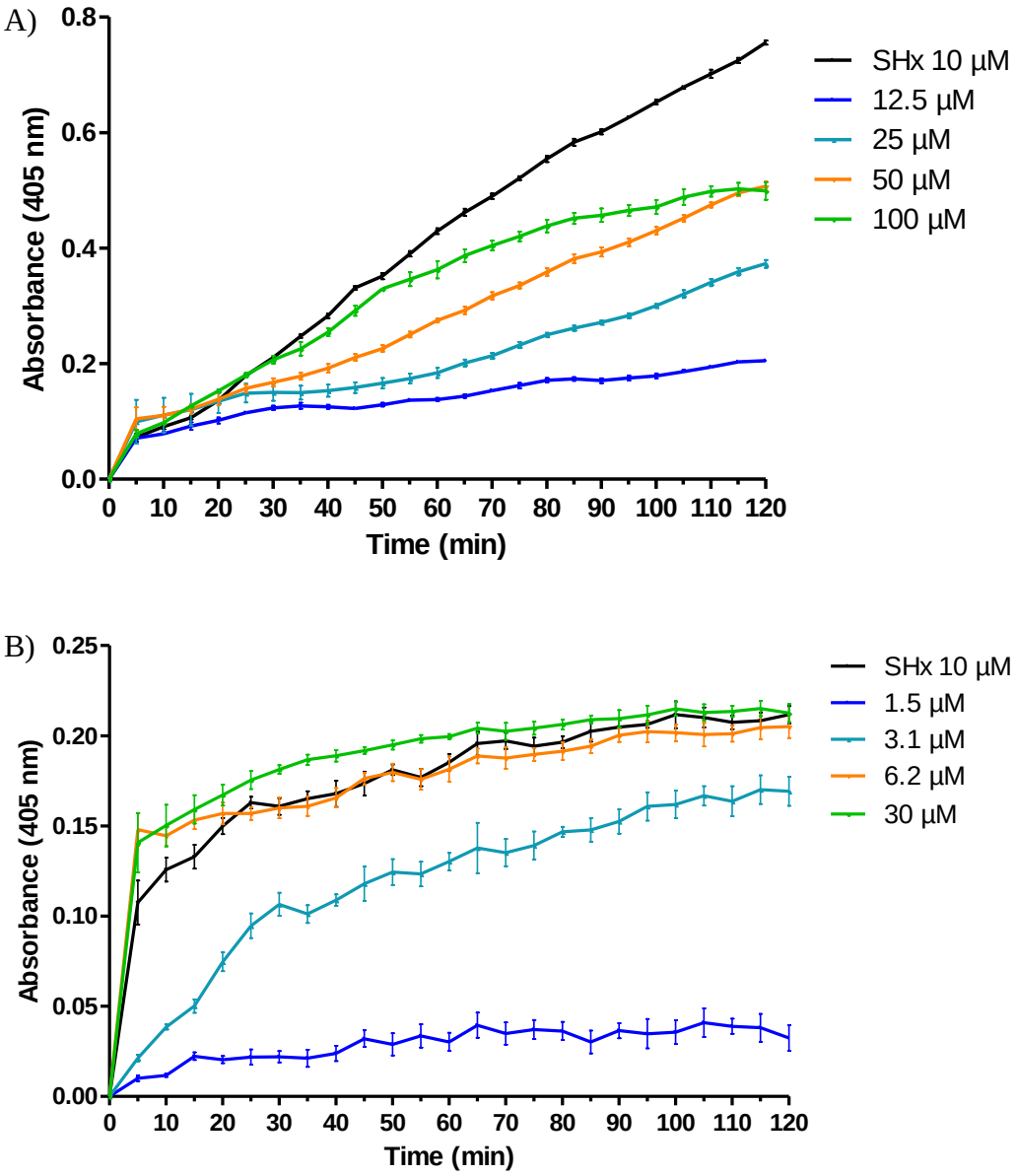

Figure 28: Temporin-SHe-induced permeabilization of bacterial cytoplasmic membranes (*E. coli* and *S. aureus*). Different concentrations of temporin-SHe were incubated with *E. coli* ML-35p (A) or *S. aureus* ST1065 (B), and hydrolysis of extracellular ONPG by cytoplasmic β-galactosidase was monitored during 120 min by measuring the absorbance of ONP at 405 nm. Temporin-SHx (black curve), a potent temporin-SHa analog, was used as positive control. Absorbance values are the mean ± S.E.M. of quadruplicates from a representative experiment.

Time-dependent killing of Gram-negative and Gram-positive bacteria

We also studied the rate of killing of temporin-SHe and -SHd against *E. coli* ATCC 25922 and *S. aureus* ST1065, in order to observe if membrane permeabilization and bacterial death were correlated. In this assay, a final peptide concentration of two-

fold above the MIC was used for each strain. The figure 29 revealed that temporin-SHe kills more efficiently Gram-positive, as well as Gram-negative bacteria, compared to temporin-SHd. Indeed, temporin-SHe rapidly kills (5 min) *S. aureus* bacteria, whereas only a slight reduction in the number of viable bacteria (26%) was obtained with temporin-SHd after 120 min of incubation (figure 29 D). We observed a much lower killing effect of temporin-SHe with Gram-negative bacteria (figure 29 A). However, although this peptide was less active (MIC = 25 µM) than temporin-SHd (MIC = 5 µM) against *E. coli* ATCC 25922, complete killing was achieved after 90 min, while only 12% reduction was obtained for temporin-SHd after 120 min (figure 29 A-B). These results indicate that there is a direct correlation between the kinetics of bacterial killing and membrane permeabilization.

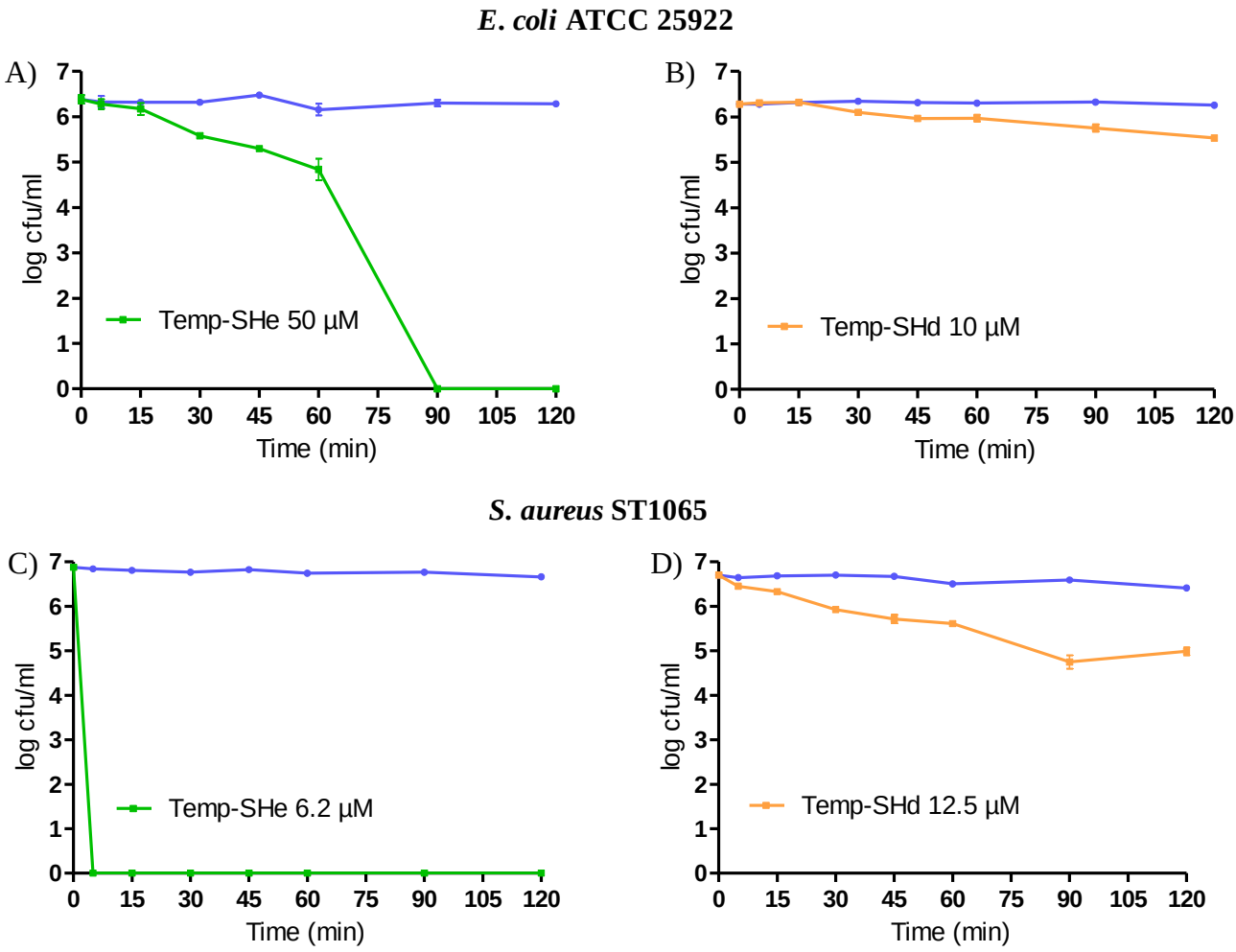

Figure 29: Time-dependent killing of Gram-negative (*E. coli* ATCC 25922) and Gram-positive (*S. aureus* ST1065) strains induced by temporin-SHe (A and C) and temporin-SHd (B and D). Bacteria (10^6 cfu/ml) were resuspended in PBS and incubated with peptide at concentrations two-fold above the MIC for *E. coli* (SHe: 50 µM, SHd: 10 µM) and *S. aureus* (SHe: 6.2 µM, SHd: 12.5 µM). Control was obtained with bacteria incubated in PBS without peptide (blue curve). The values are the mean ± S.E.M. of triplicates from a representative experiment.

DISCUSSION

During a first part of my training, I was interested in the identification of novel AMPs from skin secretions of the hylid frog *Trachycephalus resinifictrix*, which belongs to the subfamily Hylinae containing 646 species. Nowadays, only eight AMPs were identified from frogs of this subfamily, including 4 pseudins (23-24 amino acid residues), 1 hylaseptin/2 hylains (14 residues) and 1 hylin (18 residues). Moreover, surprisingly, no cDNA encoding AMP precursors were characterized. So, we attempt also to clone the precursors of AMPs present in the skin secretions of *T. resinifictrix*.

This frog has the particularity to secrete a milky and viscous resin from its skin, thus rendering difficult the extraction of AMPs, but we have successfully overcome this inconvenience. Indeed, by fractionation of skin secretions and monitoring of antibacterial activity against *Staphylococcus aureus*, we were able to identified three semi-preparative HPLC fractions (25, 29 and 37) with potent bacterial growth inhibition. After analytical HPLC, only one collected peak of the fraction 25 (peak 6) revealed potent growth-inhibitory activity. Despite the fact that interesting molecular species ($[M+H]^+$ = 1000-1900 Da) were revealed in this peak by MALDI-TOF mass spectrometry analysis, we didn't get any primary sequence after tandem mass spectrometry (MS/MS) due to small amounts of peptides in the sample. Therefore, it will be necessary to concentrate the peptide material in the fraction 25, as well as fractions 29 and 37, using the same protocol of extraction and purification but with a much higher amount of skin secretions. During my internship, I didn't have enough time for that. Moreover, it will be also interesting to extract AMPs from the entire skin.

We attempted to amplify AMP precursor cDNAs by PCR using different sets of specific primers designed to conserved regions of AMP precursors of the dermaseptin superfamily. Unfortunately, after cloning and sequence analysis of numerous clones of plasmid DNA, no AMP precursor was identified. The team has previously cloned AMP precursors from the skin exudate of *Phyllomedusa sauvagii* (hylid frog) but it is possible for the skin exudate of *T. resinifictrix* that there is too low amount or no mRNA. So, it will be necessary to sacrify a frog specimen to extract mRNA from the skin. We also cannot exclude the possibility that AMP precursors from frogs of the subfamily are not so well conserved. Therefore, it will be essential to design degenerated primers from alignment of several AMP precursors of hylid frogs. If no results are obtained, we will study another frog species of the Hylinae subfamily.

During the second part of my training, I studied AMPs of ranid frogs, and particularly small hydrophobic and cationic peptides of a family called Temporin [1]. Although these AMPs were mainly characterized from Eurasian and North American frog species, six novel temporins were also identified by the team from a North African frog (*Pelophylax saharica*), for the first time [72, 76]. Among these six temporins-SH (SHa to SHf, SH for *saharica*), only temporin-SHe remained unstudied. Therefore, in this project, my objective was to characterize the structure and function of temporin-SHe. I have also compared the properties of temporin-SHe and temporin-SHd because these peptides share high identity (76.5%) and temporin-SHd is a well-characterized paralog [77].

Circular dichroism spectroscopy studies revealed that temporin-SHe adopts a well-defined α-helical structure, preferentially when bound to anionic model membranes. This was also observed with temporin-SHd [77]. In contrast to many linear α-helical AMPs, the Schiffer-Edmundson helical-wheel projections of these two peptides showed a non-amphipathic structure with no well-separated polar and apolar faces. When the peptide-lipid molar ratio was increased up to 1:50, we observed from calorimetric data (DSC) that temporin-SHe perturbs strongly the membrane of anionic model vesicles with disappearance of the pretransition peak and alteration of the main transition peak (existence of two components). The loss of the pretransition is a consequence of the peptide interaction with phospholipid headgroups which increase the spacing between them, thus eliminating the driving force for the formation of a rippled gel phase. The shift of the temperature (Tm) of the main phase transition toward higher values indicates a rigidification of the membrane, whereas the apparition of a second peak at the right wing of the main transition peak (ratio 1:50) indicates regions of two coexisting phases, one peptide-rich (higher temperature) and the other peptide-poor (lower temperature) [78, 81]. This gradual phase segregation between these two domains may eventually lead to membrane disruption [78].

Like temporin-SHd, we have shown that temporin-SHe has potent broad-spectrum activity, acting against both Gram-positive (MIC = 1.5-12.5 µM) and Gram-negative bacteria, yeasts (*S. cerevisiae*, MIC = 12.5 µM), as well as against the extracellular promastigote form of the human parasite *Leishmania* (IC_{50} ~ 10 µM). The bacterial activity against Gram-negative strains was lower (MIC = 25-60 µM). Although the spectrum of activity of both temporins were quite similar, *Pseudomonas aeruginosa*

(MIC = 60 µM) and *Candida parapsilosis* (MIC = 50 µM) were more susceptible to temporin-SHe, while these strains were resistant to temporin-SHd. *P. aeruginosa* is an opportunistic human bacteria responsible of biofilm formation in medical tools [82]. Interestingly, temporin-SHe, as well as temporin-SHd, are active against antibiotic-multiresistant *S. aureus* (ATCC 43300 and ATCC BAA-44) with the same order of magnitude as non-resistant *S. aureus* strains (ST1065 and ATCC 25923). This emphasizes the original mode of action (membranolytic mechanism) of these AMPs compared to conventional antibiotics and also indicates that temporins are promising candidates in the fight against antibiotic-resistant pathogens. Another interesting result is that temporin-SHe is an additional temporin with antiparasitic activity against *Leishmania*. Only four temporins (A, B, SHa and SHd) were previously shown to have such activity [71, 72, 77] and very few AMPs of other families are active [38, 83]. Like temporin-SHd, temporin-SHe is active against different *Leishmania* species responsible of visceral (*L. infantum*), cutaneous (*L. major*) and muco-cutaneous (*L. braziliensis*) leishmaniasis.

We have shown that temporin-SHe is three-fold more cytotoxic than temporin-SHd toward human monocytes. This can be explained by the higher intrinsic hydrophobicity of temporin-SHe since it is known that increasing the hydrophobic character leads to more cytotoxic AMPs [84] and that hydrophobic interaction play a major role in the activity of peptides with PC-rich membranes [85]. This preliminary study of cytotoxicity needs to be extended on other cells, such as erythrocytes or macrophages (the host cells of *Leishmania*), for example.

In order to investigate the mode of action of temporin-SHe, we have analyzed the effect of this peptide on the cytoplasmic membrane of bacteria (permeabilization assay) and its ability to kill bacteria. With two-fold concentration above the MIC, we observed a complete killing which was very rapid (within 5 min) for the Gram-positive *S. aureus* and much lower (90 min) for the Gram-negative *E. coli*. Temporin-SHe was more efficient than temporin-SHd because for the latter, no complete killing occurred (*S. aureus* and *E. coli*) after 120 min of incubation with a concentration two-fold above the MIC. However, Abbassi/Raja and co-workers have shown for temporin-SHd that a three-fold concentration above the MIC (20 µM) was effective to induce rapid (15 min) and complete killing of *S. aureus*, with also rapid permeabilization of the cytoplasmic

membrane [77]. Thus, a peptide concentration threshold is needed for rapid killing of bacteria by AMP.

In addition, temporin-SHe was able to permeabilize the bacterial cytoplasmic membrane (*S. aureus* and *E. coli*) in a time- and concentration-dependent manner. The kinetics of membrane permeabilization was correlated to the bacterial killing. We observed that even at concentrations below the MIC membrane permeability occurred but does not cause bacterial lysis. This could be explained by the two-state model [86]. In this model, peptide has two physical states of binding to the lipid bilayer, one at low peptide/lipid ratios (P/L) and another at a high P/L. When a threshold ratio is reached, the peptide tends to form a stable multi-pore state, whereas the few pores formed below the threshold concentration are usually unstable [86]. However, according to several studies (reviewed in [87]), including those of the laboratory [76, 78], only the first physical state (lower concentrations) fits into the mechanism of action commonly accepted for temporins. These results indicate that temporins rather act by a carpet-like mechanism. In fact, at low temporin/lipid ratio, peptide induces the formation of transient, toroidal lipid-peptide pores, with possibility of peptide translocation into the cell. At a higher temporin/lipid ratio, peptide induces membrane disruption by a detergent-like effect, as it has been demonstrated for temporin-SHf [76] (figure 30).

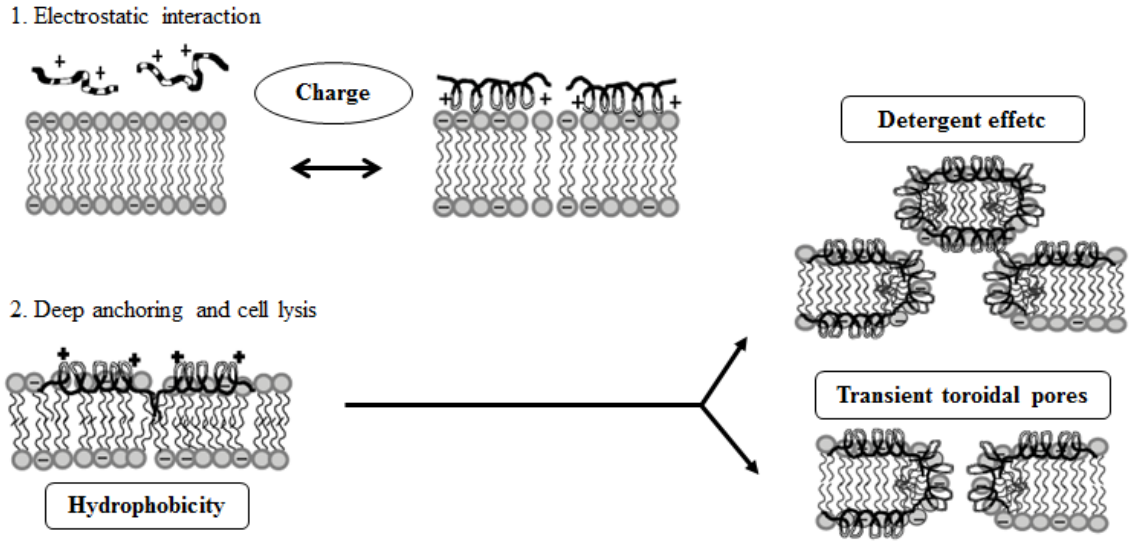

Figure 30: Hypothetical mechanism of action of temporins. The first step involves reversible electrostatic interactions of the cationic peptide with the negatively charged membrane (carpet-like mechanism). In the second step, the hydrophobicity of the peptide allows its insertion into the hydrophobic core of the bilayer and then i) at low concentrations, peptide induces the formation of transient toroidal lipid-peptide pores with possibility of peptide translocation into the cell; ii) at higher concentrations, peptide provokes membrane micellization by a detergent-like effect. The black area of the AMP corresponds to the hydrophobic region and the white area to the cationic region of the peptide. Gray circles of the membrane correspond to polar headgroups and squiggly lines to the acyl chains of the phospholipids (adapted from [87]).

CONCLUSION

Skin secretions of the frog *T. resinifictrix* contain probably AMPs because after fractionation we were able to detect HPLC peaks at 220 nm displaying antibacterial activity against *S. aureus*. We need now to characterize these AMPs.

The structural characterization of temporin-SHe revealed that this peptide adopts a well-defined α-helical conformation when bound to negatively charged model membranes. Temporin-SHe interacts with the phospholipid headgroups of these model membranes and induces membrane perturbations probably by insertion into the hydrophobic core of the phospholipid bilayer. The membranolytic activity of temporin-SHe was revealed by killing of bacteria, as well as Gram-positive and Gram-negative, and concomitant permeabilization of the bacterial cytoplasmic membrane. This activity, which is concentration-dependent, involves probably the formation of either transient toroidal lipid-peptide pores (at low peptide concentration) or membrane micellization (detergent-like effect at a higher peptide concentration). Temporin-SHe, as well as temporin-SHd and -SHa, are particularly interesting AMPs with potent and broad-spectrum activity against a wide range of microorganisms, including both Gram-positive and Gram-negative bacteria, yeasts, fungi and human protozoa. Moreover, these peptides display high potency toward antibiotic-multiresistant strains.

Therefore, temporins-SH represent good templates for the development of therapeutic antimicrobial agents with new mode of action. Today, the antiparasitic mechanism of action of AMPs is unknown and very few AMPs are active against protozoa. So, our results indicate that temporin-SHe represents a good additional tool to analyze this mechanism.

REFERENCES

1. Mangoni, M. L. (2006) Temporins, anti-infective peptides with expanding properties. *Cell Mol Life Sci 63*, 1060-1069.

2. Hancock, R. E. W., and Diamond, G. (2000) The role of cationic antimicrobial peptides in innate host defences. *Trends Microbiol 8*, 402-410.

3. Zasloff, M. (2002) Antimicrobial peptides of multicellular organisms. *Nature 415*, 389-395.

4. Wang, G., Li, X. and Wang, Z. (2009) APD2 : the updated antimicrobial peptide database and its application in peptide design. *Nucleic Acids Res 37*, D933-D937.

5. Clarke, B. T. (1997) The natural history of amphibian skin secretions, their normal functioning and potential medical applications. *Biol Rev 72*, 365-379.

6. Lazarus, L. H., and Attila, M. (1993) The toad, ugly and venomous, wears yet a precious jewel in his skin. *Prog Neurobiol 41*, 473-507.

7. Simmaco, M., Mignogna, G., and Barra, D. (1998) Antimicrobial peptides from amphibian skin: What do they tell us? *Biopolymers 47*, 435-450.

8. Amiche, M., Delfour, A., and Nicolas, P. (1999) La peau des grenouilles, un mini-laboratoire pour les biotechnologies. In *Revue du Palais de la découverte*, pp 11-21.

9. Frost, D. R. (2011) Amphibian Species of the World: an Online Reference. version 5.5. In *American Museum of Natural History*.

10. Nascimento, A. C., Fontes, W., Sebben, A., and Castro, M. S. (2003) Antimicrobial peptides from anurans skin secretions. *Protein Pept Lett 10*, 227-238.

11. Barra, D., and Simmaco, M. (1995) Amphibian Skin - a Promising Resource for Antimicrobial Peptides. *Trends Biotechnol 13*, 205-209.

12. Lacombe, C. (2000) Peptide secretion in the cutaneous glands of South American tree frog: an ultrastructural study. *Eur J Cell Biol 79*, 631-641.

13. Azevedo Calderon, L. d., Silva, A. d. A. E., Ciancaglini, P., and Stábeli, R. G. (2010) Antimicrobial peptides from Phyllomedusa frogs: from biomolecular diversity to potential nanotechnologic medical applications. *Amino Acids 40*, 29-49.

14. Toledo, R. C., and Jared, C. (1995) Cutaneous granular glands and amphibian venoms. *Comp Biochem Physiol 111A*, 1-29.

15. El Amri, C., and Nicolas, P. (2008) Plasticins: membrane-damaging peptides with 'chameleon-like' properties. *Cell Mol Life Sci 65*, 895-909.

16. Delfino, G., Brizzi, R., Nosi, D., and Terreni, A. (2002) Serous Cutaneous Glands in New World Hylid Frogs: An Ultrastructural Study on Skin Poisons Confirms Phylogenetic Relationships Between *Osteopilus septentrionalis* and *Phrynohyas venulosa*. *J Morphol 253*, 176-186.

17. Nicolas, P., and El Amri, C. (2009) The dermaseptin superfamily: a gene-based combinatorial library of antimicrobial peptides. *Biochim Biophys Acta 1788*, 1537-1550.

18. Nicolas, P., and Amiche, M. (1999) Les précurseurs des dermaseptines: une boÎte de Pandore. In *Médecine/sciences*, pp 1443-1447.

19. Bevins, C. L., and Zasloff, M. (1990) Peptides from frog skin. *Annu Rev Biochem 59*, 395-414.

20. Andreu, D., and Rivas, L. (1998) Animal antimicrobial peptides: an overview. *Biopolymers 47*, 415-433.

21. Peschel, A., and Sahl, H. G. (2006) The co-evolution of host cationic antimicrobial peptides and microbial resistance. *Nat Rev Microbiol 4*, 529-536.

22. Nicolas, P., Vanhoye, D., and Amiche, M. (2003) Molecular strategies in biological evolution of antimicrobial peptides. *Peptides 24*, 1669-1680.

23. Amiche, M., Seon, A. A., Pierre, T. N., and Nicolas, P. (1999) The dermaseptin precursors: a protein family with a common preproregion and a variable C-terminal antimicrobial domain. *FEBS Lett 456*, 352-356.

24. Vanhoye, D., Bruston, F., Nicolas, P., and Amiche, M. (2003) Antimicrobial peptides from hylid and ranin frogs originated from a 150-million-year-old ancestral precursor with a conserved signal peptide but a hypermutable antimicrobial domain. *Eur J Biochem 270*, 2068-2081.

25. Amiche, M., Ducancel, F., Mor, A., Boulain, J. C., Menez, B., and Nicolas, P. (1994) Precursors of Vertebrate Peptide Antibiotics Dermaseptin b and Adenoregulin Have Extensive Sequence Identities with Precursors of Opioid Peptides Dermorphin, Dermenkephalin, and Deltorphins. *J Biol Chem 269*, 17847-17852.

26. Yeaman, M. R., and Yount, N. Y. (2003) Mechanisms of antimicrobial peptide action and resistance. *Pharmacol Rev 55*, 27-55.

27. Hancock, R. E. (1997) Peptide antibiotics. *Lancet 349*, 418-422.

28. Conlon, J. M. (2010) The contribution of skin antimicrobial peptides to the system of innate immunity in anurans. *Cell Tissue Res 343*, 201-212.

29. Brogden, K. A. (2005) Antimicrobial peptides: pore formers or metabolic inhibitors in bacteria? *Nat Rev Microbiol 3*, 238-250.

30. Pukala, T. L., Bowie, J. H., Maselli, V. M., Musgrave, I. F., and Tyler, M. J. (2006) Host-defence peptides from the glandular secretions of amphibians: structure and activity. *Nat Prod Rep 23*, 368-393.

31. Haney, E. F., Hunter, H. N., Matsuzaki, K., and Vogel, H. J. (2009) Solution NMR studies of amphibian antimicrobial peptides: linking structure to function? *Biochim Biophys Acta 1788*, 1639-1655.

32. Bulet, P., Stöcklin, R., and Menin, L. (2004) Anti-microbial peptides: from invertebrates to vertebrates. *Immunol Rev 198*, 169-184.

33. Rinaldi, A. C. (2002) Antimicrobial peptides from amphibian skin: an expanding scenario. *Curr Opin Chem Biol 6*, 799-804.

34. Shai, Y. (2002) Mode of action of membrane active antimicrobial peptides. *Biopolymers 66*, 236-248.

35. Epand, R. M., and Vogel, H. J. (1999) Diversity of antimicrobial peptides and their mechanisms of action. *Biochim Biophys Acta 1462*, 11-28.

36. Shai, Y. (1999) Mechanism of the binding, insertion and destabilization of phospholipid bilayer membranes by α-helical antimicrobial and cell non-selective membrane-lytic peptides. *Biochim Biophys Acta 1462*, 55-70.

37. Shai, Y., and Oren, Z. (2001) From "carpet" mechanism to de-novo designed diastereomeric cell-selective antimicrobial peptides. *Peptides 22*, 1629-1641.

38. Rivas, L., Luque-Ortega, J. R., and Andreu, D. (2009) Amphibian antimicrobial peptides and Protozoa: lessons from parasites. *Biochim Biophys Acta 1788*, 1570-1581.

39. Yang, L., Harroun, T. A., Weiss, T. M., Ding, L., and Huang, H. W. (2001) Barrel-stave Model or Toroidal Model? A case study on melittin pores. *Biophys J 81*, 1475-1485.

40. Tossi, A., Sandri, L., and Giangaspero, A. (2000) Amphipathic, alpha-helical antimicrobial peptides. *Biopolymers 55*, 4-30.

41. Mor, A., and Nicolas, P. (1994) Isolation and structure of novel defensive peptides from frog skin. *Eur J Biochem 219*, 145-154.

42. Conlon, J. M., Woodhams, D. C., Raza, H., Coquet, L., Leprince, J., Jouenne, T., Vaudry, H., and Rollins-Smith, L. A. (2007) Peptides with differential cytolytic activity from skin secretions of the lemur leaf frog Hylomantis lemur (Hylidae: Phyllomedusinae)☆. *Toxicon 50*, 498-506.

43. Vanhoye, D., Bruston, F., El Amri, S., Ladram, A., Amiche, M., and Nicolas, P. (2004) Membrane association, electrostatic sequestration, and cytotoxicity of Gly-Leu-rich peptide orthologs with differing functions. *Biochemistry 43*, 8391-8409.

44. Amiche, M., Seon, A. A., Wroblewski, H., and Nicolas, P. (2000) Isolation of dermatoxin from frog skin, an antibacterial peptide encoded by a novel member of the dermaseptin genes family. *Eur J Biochem 267*, 4583-4592.

45. Pierre, T. N., Seon, A. A., Amiche, M., and Nicolas, P. (2000) Phylloxin, a novel peptide antibiotic of the dermaseptin family of antimicrobial/opioid peptide precursors. *Eur J Biochem 267*, 370-378.

46. Thompson, A. H., Bjourson, A. J., Orr, D. F., Shaw, C., and McClean, S. (2007) Amphibian skin secretomics: application of parallel quadrupole time-of-flight mass spectrometry and peptide precursor cDNA cloning to rapidly characterize the skin secretory peptidome of Phyllomedusa hypochondrialis azurea: discovery of a novel peptide family, the hyposins. *J Proteom Res 6*, 3604-3613.

47. Lequin, O., Ladram, A., Chabbert, L., Bruston, F., Convert, O., Vanhoye, D., Chassaing, G., Nicolas, P., and Amiche, M. (2006) Dermaseptin S9, an alpha-helical antimicrobial peptide with a hydrophobic core and cationic termini. *Biochemistry 45*, 468-480.

48. Rozek, T., Wegener, K. L., Bowie, J. H., Olver, I. N., Carver, J. A., Wallace, J. C., and Tyler, M. J. (2000) The antibiotic and anticancer active aurein peptides from the Australian Bell Frogs Litoria aurea and Litoria raniformis the solution structure of aurein 1.2. *Eur J Biochem 267*, 5330-5341.

49. Wong, H., Bowie, J. H., and Carver, J. A. (1997) The solution structure and activity of caerin 1.1, an antimicrobial peptide from the Australian green tree frog, Litoria spzendida. *Eur J Biochem 247*, 545-557.

50. Wegener, K. L., Wabnitz, P. A., Carver, J. A., Bowie, J. H., Chia, B. C., Wallace, J. C., and Tyler, M. J. (1999) Host defence peptides from the skin glands of the Australian blue mountains tree-frog Litoria citropa. Solution structure of the antibacterial peptide citropin 1.1. *Eur J Biochem 265*, 627-637.

51. Wegener, K. L., Brinkworth, C. S., Bowie, J. H., Wallace, J. C., and Tyler, M. J. (2001) Bioactive dahlein peptides from the skin secretions of the Australian aquatic frog Litoria dahlii: sequence determination by electrospray mass spectrometry. *Rapid Commun Mass Spectrom 15*, 1726-1734.

52. Rozek, T., Waugh, R. J., Steinborner, S. T., Bowie, J. H., Tyler, M. J., and Wallace, J. C. (1998) The maculatin peptide from the skin glands of the tree frog Litoria genimaculata. A comparison of the structures and antibacterial activities of maculatin 1.1 and caerin 1.1. *J Pept Sci 4*, 111-115.

53. Amiche, M., Ladram, A., and Nicolas, P. (2008) A consistent nomenclature of antimicrobial peptides isolated from frogs of the subfamily Phyllomedusinae. *Peptides 29*, 2074-2082.

54. Olson III, L., Soto, A. M., Knoop, F. C., and Conlon, J. M. (2001) Pseudin-2: An antimicrobial peptide with low hemolytic activity from the skin of the Paradoxical Frog. *Biochem Biophys Res Commun 288*, 1001-1005.

55. Prates, M. V., Sforca, M. L., Regis, W. C., Leite, J. R., Silva, L. P., Pertinhez, T. A., Araujo, A. L., Azevedo, R. B., Spisni, A., and Bloch, C., Jr. (2004) The NMR-derived solution structure of a new cationic antimicrobial peptide from the skin secretion of the anuran Hyla punctata. *J Biol Chem 279*, 13018-13026.

56. Wu, J., Liu, H., Yang, H., Yu, H., You, D., Ma, Y., Ye, H., and Lai, R. (2011) Proteomic analysis of skin defensive factors of tree frog Hyla simplex. *J Proteome Res 10*, 4230-4240.

57. Castro, M. S., Ferreira, T. C., Cilli, E. M., Crusca, E., Jr., Mendes-Giannini, M. J., Sebben, A., Ricart, C. A., Sousa, M. V., and Fontes, W. (2009) Hylin a1, the first cytolytic peptide isolated from the arboreal South American frog Hypsiboas albopunctatus ("spotted treefrog"). *Peptides 30*, 291-296.

58. van Zoggel, H., Hamma-Kourbali, Y., Galanth, C., Ladram, A., Nicolas, P., Courty, J., Amiche, M., and Delbe, J. (2010) Antitumor and angiostatic peptides from frog skin secretions. *Amino Acids*.

59. Abdel-Wahab, Y. H., Power, G. J., Flatt, P. R., Woodhams, D. C., Rollins-Smith, L. A., and Conlon, J. M. (2008) A peptide of the phylloseptin family from the skin of the frog Hylomantis lemur (Phyllomedusinae) with potent in vitro and in vivo insulin-releasing activity. *Peptides 29*, 2136-2143.

60. Apponyi, M., Pukala, T., Brinkworth, C., Maselli, V., Bowie, J., Tyler, M., Booker, G., Wallace, J., Carver, J., and Separovic, F. (2004) Host-defence peptides of Australian anurans: structure, mechanism of action and evolutionary significance. *Peptides 25*, 1035-1054.

61. VanCompernolle, S. E., Taylor, R. J., Oswald-Richter, K., Jiang, J., Youree, B. E., Bowie, J. H., Tyler, M. J., Conlon, J. M., Wade, D., Aiken, C., Dermody, T. S., KewalRamani, V. N., Rollins-Smith, L. A., and Unutmaz, D. (2005) Antimicrobial Peptides from Amphibian Skin Potently Inhibit Human Immunodeficiency Virus Infection and Transfer of Virus from Dendritic Cells to T Cells. *J Virol 79*, 11598-11606.

62. Abdel-Wahab, Y. H. A., Power, G. J., Ng, M. T., Flatt, P. R., and Conlon, J. M. (2008) Insulin-releasing properties of the frog skin peptide pseudin-2 and its [Lys18]-substituted analogue. *Biol Chem 389*, 143-148.

63. Rotem, S., and Mor, A. (2009) Antimicrobial peptide mimics for improved therapeutic properties. *Biochim Biophys Acta 1788*, 1582-1592.

64. Zampa, M. F., Araújo, I. M. S., Costa, V., Nery Costa, C. H., Santos, J. R., Zucolotto, V., Eiras, C., and Leite, J. R. S. A. (2009) Leishmanicidal Activity and Immobilization of dermaseptin 01 antimicrobial peptides in ultrathin films for nanomedicine applications. *Nanomedicine 5*, 352-358.

65. Wang, H., Xu, K., Liu, L., Tan, J. P. K., Chen, Y., Li, Y., Fan, W., Wei, Z., Sheng, J., Yang, Y.-Y., and Li, L. (2010) The efficacy of self-assembled cationic antimicrobial peptide nanoparticles against Cryptococcus neoformans for the treatment of meningitis. *Biomaterials 31*, 2874-2881.

66. Simmaco, M., Mignogna, G., Canofeni, S., Miele, R., Mangoni, M. L., and Barra, D. (1996) Temporins, antimicrobial peptides from the European red frog *Rana temporaria*. *Eur J Biochem 242*, 788-792.

67. Marenah, L., Flatt, P. R., Orr, D. F., Shaw, C., and Abdel-Wahab, Y. H. (2006) Skin secretions of Rana saharica frogs reveal antimicrobial peptides esculentins-1 and -1B and brevinins-1E and -2EC with novel insulin releasing activity. *J Endocrinol 188*, 1-9.

68. Giacometti, A., Cirioni, O., Kamysz, W., D'Amato, G., Silvestri, C., Del Prete, M. S., Licci, A., Lukasiak, J., and Scalise, G. (2005) In vitro activity and killing effect of temporin A on nosocomial isolates of Enterococcus faecalis and interactions with clinically used antibiotics. *J Antimicrob Chemother 55*, 272-274.

69. Wade, D., Silberring, J., Soliymani, R., Heikkinen, S., Kilpelainen, I., Lankinen, H., and Kuusela, P. (2000) Antibacterial activities of temporin A analogs. *FEBS Lett 479*, 6-9.

70. Rinaldi, A. C., Mangoni, M. L., Rufo, A., Luzi, C., Barra, D., Zhao, H., Kinnunen, P. K., Bozzi, A., Di Giulio, A., and Simmaco, M. (2002) Temporin L: antimicrobial, haemolytic and cytotoxic activities, and effects on membrane permeabilization in lipid vesicles. *Biochem J 368*, 91-100.

71. Mangoni, M. L., Saugar, J. M., Dellisanti, M., Barra, D., Simmaco, M., and Rivas, L. (2005) Temporins, small antimicrobial peptides with leishmanicidal activity. *J Biol Chem 280*, 984-990.

72. Abbassi, F., Oury, B., Blasco, T., Sereno, D., Bolbach, G., Nicolas, P., Hani, K., Amiche, M., and Ladram, A. (2008) Isolation, characterization and molecular cloning of new temporins from the skin of the North African ranid Pelophylax saharica. *Peptides 29*, 1526-1533.

73. Chen, Q., Wade, D., Kurosaka, K., Wang, Z. Y., Oppenheim, B. J., and Yang, D. (2004) Temporin a and related frog antimicrobial peptides use formyl peptide receptor-like 1 as a receptor to chemoattract phagocytes. *J Immunol 173*, 2652-2659.

74. Zhao, H., and Kinnunen, P. K. (2003) Modulation of the activity of secretory phospholipase A2 by antimicrobial peptides. *Antimicrob Agents Chemother 47*, 965-971.

75. Conlon, J. M. (2008) Reflections on a systematic nomenclature for antimicrobial peptides from the skins of frogs of the family Ranidae. *Peptides 29*, 1815-1819.

76. Abbassi, F., Lequin, O., Piesse, C., Goasdoue, N., Foulon, T., Nicolas, P., and Ladram, A. (2010) Temporin-SHf, a New Type of Phe-rich and Hydrophobic Ultrashort Antimicrobial Peptide. *J Biol Chem 285*, 16880-16892.

77. Abbassi, F*., Raja, Z*., Oury, B., Gazanion, E., Piesse, C., Sereno, D., Foulon, T., Nicolas, P., and Ladram, A. Antibacterial and leishmanicidal activities of temporin-SHd, a 17-residue long membrane-damaging peptide. *Submitted to Antimicrob Agents Chemother *These authors contributed equally to this work.*

78. Abbassi, F., Galanth, C., Amiche, M., Saito, K., Piesse, C., Zargarian, L., Hani, K., Nicolas, P., Lequin, O., and Ladram, A. (2008) Solution structure and model membrane interactions of temporins-SH, antimicrobial peptides from amphibian skin. A NMR spectroscopy and differential scanning calorimetry study. *Biochemistry 47*, 10513-10525.

79. Tapley, B., and Bradfield, K. S. (2007) Mission golden-eyed tree frog *Trachycephalus resinifictrix DWCT*.

80. Eeman, M., and Deleu, M. (2010) From biological membranes to biomimetic model membranes. *Biotechnol. Agron. Soc. Environ. 14*, 719-736.

81. Lohner, K., Latal, A., Lehrer, R. I., and Ganz, T. (1997) Differential scanning microcalorimetry indicates that human defensin, HNP-2, interacts specifically with biomembrane mimetic systems. *Biochemistry 36*, 1525-1531.

82. Batoni, G., Maisetta, G., Brancatisano, F. L., Esin, S., and Campa, M. (2011) Use of Antimicrobial Peptides Against Microbial Biofilms: Advantages and Limits. *Curr Med Chem 18*, 256-279.

83. Cobb, S. L., and Denny, P. W. (2010) Antimicrobial peptides for leishmaniasis. *Curr Opin Investig Drugs 11*, 868-875.

84. Conlon, J. M., Al-Ghaferi, N., Abraham, B., and Leprince, J. (2007) Strategies for transformation of naturally-occurring amphibian antimicrobial peptides into therapeutically valuable anti-infective agents. *Methods 42*, 349-357.

85. Wieprecht, T., Dathe, M., Beyermann, M., Krause, E., Maloy, W. L., MacDonald, D. L., and Bienert, M. (1997) Peptide hydrophobicity controls the activity and selectivity of magainin 2 amide in interaction with membranes. *Biochemistry 36*, 6124-6132.

86. Huang, H. W. (2000) Action of antimicrobial peptides: two-state model. *Biochemistry 39*, 8347-8352.

87. Amiche, M., and Galanth, C. (2011) Dermaseptins as Models for the Elucidation of Membrane-Acting Helical Amphipathic Antimicrobial Peptides. *Curr Pharm Biotechno 12*, 1184-1193.